Available online at www.sciencedirect.com
ScienceDirect
Bioorganic & Medicinal Chemistry 14 (2006) 7258–7281
Bioorganic & Medicinal Chemistry

Synthesis and biological activity of tricyclic arylo-imidazo-, pyrimido-, and diazepinopurinediones

Anna Drabczyńska,[a] Christa E. Müller,[b] Svenja K. Lacher,[b] Britta Schumacher,[b] Janina Karolak-Wojciechowska,[c] Antony Nasal,[d] Piotr Kawczak,[d] Olga Yuzlenko,[a] Elżbieta Pękala[a] and Katarzyna Kieć-Kononowicz[a,*]

[a]*Jagiellonian University, Medical College, Faculty of Pharmacy, Department of Technology and Biotechnology of Drugs, Medyczna 9, Pl 30-688 Kraków, Poland*
[b]*Pharmaceutical Institute Poppelsdorf, University of Bonn, Kreuzbergweg 26, D 53115 Bonn, Germany*
[c]*Institute of General and Ecological Chemistry, Technical University of Łódź, Żwirki 36, Pl 90-924 Łódź, Poland*
[d]*Department of Biopharmaceutics and Pharmacodynamics, Medical University of Gdańsk, Hallera 107, Pl 80-416 Gdańsk, Poland*

Received 23 January 2006; revised 20 June 2006; accepted 23 June 2006
Available online 17 July 2006

Abstract—Syntheses and physicochemical properties of N-aryl-substituted imidazo-, pyrimido-, and 1,3-diazepino[2,1-*f*]purinediones are described. These derivatives were synthesized by the cyclization of 7-haloalkyl-8-bromo-1,3-dimethyl- or 1,3-dipropyl-xanthine derivatives with corresponding arylamines. The obtained compounds (**1**–**40**), which can be envisaged as sterically fixed and configurationally stable analogs of 8-styrylxanthines, were evaluated for their affinity to adenosine A_1 and A_{2A} receptors, the receptor subtypes that are predominant in the brain. Selected compounds were additionally investigated for affinity to the A_{2B} and A_3 receptor subtypes. Many of the compounds showed adenosine A_{2A} receptor affinity at micromolar or submicromolar concentrations and were A_{2A}-selective, for example, compound **23** with *p*-fluoro substituent displayed K_i value of 0.147 μM at the rat A_{2A} receptor and more than 170-fold-A_{2A} selectivity, compound **17** with naphthyl substituent had K_i value of 0.219 μM and a more than 114-fold-A_{2A} selectivity. The compounds were somewhat weaker and less selective at the human receptor subtypes. Elongation of the dimethyl substituent to dipropyl in xanthine moiety improved affinity but reduced selectivity. 1,3-Dimethylimidazo-, pyrimido-, and diazepinopurinediones were evaluated in vivo as anticonvulsants in MES, ScMet, TTE tests and examined for neurotoxicity in mice (ip). Substances with pyrimido ring displayed protective activity in ScMet or in MES and ScMet tests, showing also neurotoxicity. The pyrimidine annelated ring is beneficial for both receptor affinity and anticonvulsant activity.

1. Introduction

Adenosine, an endogenous modulator of a wide range of biological functions, interacts with four different (A_1, A_{2A}, A_{2B}, and A_3) cell surface receptor subtypes, belonging to the superfamily of G protein-coupled receptors. Recent studies indicate widening role for adenosine receptors (ARs) in many therapeutic areas, including immunology, the cardiovascular system, and various CNS-mediated events such as sleep, neuroprotection, and pain.[1,2]

Adenosine A_1-receptors, the first subtype identified, are widely distributed in the central nervous system and in peripheral tissues. The role of adenosine as neuroprotective agent during hypoxia and ischemic conditions seems to be mediated by the A_1 receptors. These receptors have been shown to be involved in sedative, antiseizure, and anxiolytic effects. A_1 receptors mediate cardiac depression through negative chronotropic and inotropic effects. In the kidney, activation of A_1 receptors causes vasoconstriction, inhibition of secretion, diuresis, and natriuresis.[3] A number of A_1 antagonists have been studied as novel potassium-sparing diuretics with kidney-protecting properties; in dementia and for cardiac therapy.[1,4–6]

The adenosine A_{2A} receptor plays an important role in regulating smooth and well-coordinated movement in part by modulating the activity of dopamine sensitive

Keywords: Adenosine A_1; A_{2A} receptor ligands; Arylimidazo-; Pyrimido-; Diazepinopurinediones; Anticonvulsant activity.
* Corresponding author. Tel./fax: +48 12 657 04 88; e-mail: mfkonono@cyf-kr.edu.pl

0968-0896/$ - see front matter © 2006 Elsevier Ltd. All rights reserved.
doi:10.1016/j.bmc.2006.06.052

neurons. Adenosine A_{2A} receptors are located in brain primarily in the striatum where they are co-localized with dopamine D_2 receptors. There is now accumulating evidence that adenosine A_{2A} receptor antagonists may provide a novel therapy for the treatment of Parkinson's disease with a lower risk of dyskinesias.[7,8]

Studies have shown that A_{2B} adenosine receptors present in airway mast cells mediate the bronchoconstriction response to adenosine (unique to the airways of asthmatics) and also facilitate mast cell degranulation in responses to allergen. Accordingly, selective A_{2B} AR antagonists have been suggested to be useful as potential treatment of asthma.[9] Additionally A_{2B} AR antagonists may have potential in the treatment of diabetic retinopathy, cancer, and Alzheimer's disease.[10,11]

The A_3 AR has been linked to several diseases such as cardiac ischemia, cerebral ischemia, inflammation, cancer and hence has been a primary target for new therpeutics. A_3 AR antagonists might be therapeutically useful for the acute treatment of stroke, for glaucoma, and also as antiasthmatic and antiallergic drugs.[12,13]

In the past 10 years, great efforts by medicinal chemists and pharmacologists have been devoted to the design of potent and selective ligands for adenosine receptors.[2,5,6,8,12] Annelated in various positions of the xanthine scaffold, derivatives of **I** (Fig. 1) were obtained. They contained 1,2-[14] 2,3-[14] 3,9-[15], and 1,6-[16,17] fused rings attached to the xanthine moiety, and frequently additional aryl residues were present. Such compounds were potent antagonists at the various AR subtypes.[14]

Adenosine A_{2A} receptor antagonists are divided into xanthine and non-xanthine derivatives (nitrogen polyheterocyclic systems).[18] In the group of xanthine derivatives it has been discovered that the introduction of a styryl group in the 8-position was critical in obtaining compounds endowed with selective A_{2A} receptor antagonistic properties (Fig. 1).[19,20] As a result, several 8-styryl xanthine derivatives were developed which have been extensively studied for their pharmacological properties.[21–24] **KF 17837** and **KW 6002** being chemical homologs, despite having similar in vitro profiles, appeared to have dramatically different in vivo potencies, as measured by the attenuation of haloperidol-induced catalepsy in mice, with **KW 6002** being clearly more potent.[25] This divergence in the in vivo activity may be due to differences in pharmacokinetics, pharmacodynamics, metabolism, and/or bioavailability. **KW-6002** is now undergoing phase II clinical trials for the treatment of Parkinson's disease and depression.[26,27] Since the future management of Parkinson's disease (PD) requires pharmacological agents that do not lose efficacy with disease progression or induce dyskinesia and that are free of other dopaminergic side effects, adenosine A_{2A} receptor antagonists are a novel approach to treat the illness both as monotherapy and in combination with dopaminergic drugs.[28–30] Additionally, it was suggested that selective A_{2A} AR antagonists (e.g., **KW-6002**) possess neuroprotective properties.[31] Adenosine A_{2A} receptor antagonists seem to be involved in the regulation of glutamatergic transmission,[32,33] and the hypothesis appeared that blockade of A_{2A} ARs produces anti-nociceptive effects.[34]

A series of 3,7-dimethyl-1-propargyl 8-styrylxanthine derivatives, potent and selective A_{2A} ARs antagonists, were developed by Müller et al. (e.g., **BS-DMPX**, **MSX-2**).[33–37] A major problem of A_{2A} AR antagonists is their usually low water solubility,[38] which limited their

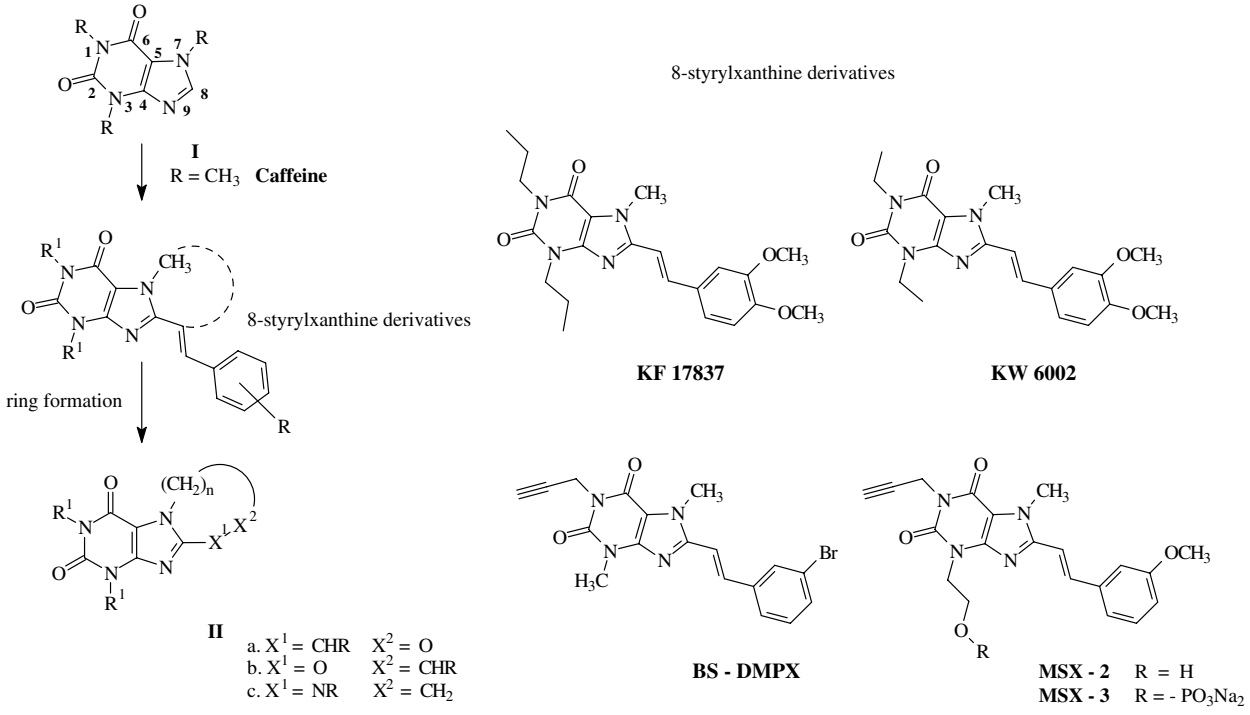

Figure 1. Xanthine (**I**), 8-styrylxanthines, and oxygen- or nitrogen-containing 7,8 annelated xanthine derivatives (**II**).

usefulness especially for in vivo studies. Therefore, Müller et al. developed water-soluble A_{2A}-selective AR antagonists (e.g., –**MSX-3**) useful as pharmacological tools.[36,37] **MSX-2** has been also prepared in tritiated form as radioligand for labeling A_{2A} ARs.[39] Several A_{2A} AR antagonists labeled with positron-emitting radionuclides have been prepared for the visualization and quantification of A_{2A} ARs using PET (positron emission tomography).[40] The main drawback specific for this class of compounds is their low stability. In dilute solution they suffer from sensitivity to photoisomerization: the active (E)-configurated 8-styrylxanthines form isomeric mixtures in which often the less active or even inactive (Z)-isomer dominates.[41,42] Furthermore, it was described that solid 8-styrylxanthines can dimerize upon exposition to daylight or irradiation with UV light. The resulting dimeric cyclobutane derivatives exhibited considerably lower A_{2A} AR affinity than their parent compounds.[41]

Our research efforts have been directed toward the study of novel selective ligands for A_1 and especially A_{2A} ARs. Various tricyclic xanthine derivatives, products of xanthine 7,8 annelation (**II**), were obtained (Fig. 1). In previous studies it was established that 7-*N*-methylxanthinyl analogs were more potent as adenosine A_{2A} receptor antagonists as well as inhibitors of MAO-B than the corresponding 7*H*-xanthinyl analogs.[31] Therefore, substitution at the 7-position was advantageous for biological activity. Based on that observation, we designed compounds that can be envisaged as constrained analogs of styrylxanthine derivatives. The new compounds could be envisaged as bioisosteric analogs of 8-styrylxanthines fixed in a biologically active configuration. However, in contrast to styrylxanthines, they cannot isomerize in solution or in solid state due to their sterically fixed structure. Thus oxygen- (**IIa**, **IIb**) and nitrogen-containing (**IIc**) annelated theophylline derivatives, products of xanthine-7,8-annelation of the general structure **II** (Fig. 1), were obtained.[14,43,44] Such tricyclic structures exhibited A_1 or A_{2A} AR antagonistic properties, in some cases selectivity to one of the above-mentioned subtypes of receptors. The investigated compounds showed anticonvulsant activity in the in vivo (MES or ScMet) tests, however the mechanism of this action was not clear. In the group of oxazolo[2,3-*f*]purinediones SAR and QSAR studies had indicated the importance of lipophilic substituents of limited size for both types of pharmacological activity.[44]

As a continuation of our research program we have now synthesized and tested at ARs a set of nitrogen-containing tricyclic structures with N-aryl moiety. Thus, imidazo-, pyrimido-, and diazepinopurinediones were designed with the aim to examine the impact of the ring size (5-, 6-, and 7-membered) and its spatial arrangement on the biological activity. Various structural modifications on the aryl group were performed. The first one was the introduction of different substituent(s) at different positions of the phenyl moiety. Substituents with hydrophilic properties (OH, OMe, and NHCOCH$_3$) were included in order to improve the water solubility of the examined compounds. More voluminous residues (naphthyl) and additional phenyl substituents were also investigated. 1,3-Dimethyl derivatives were compared with 1,3-dipropyl ones. The synthesized compounds were evaluated in vitro for their affinity to ARs and in vivo for anticonvulsant properties. Physicochemical properties of tested compounds were estimated by means of calculations as well as by experimental methods. In order to analyze three dimensional properties of this group of compounds structure elucidation was performed by means of molecular modeling and of X-ray analysis for two selected compounds.

2. Chemistry

The synthesis of tricyclic 1,3-dimethylperhydro-imidazo-, pyrimido-, and 1,3-diazepino 2,1-*f*]purinediones with aromatic substituents in the 8-, 9-, or 10-position, respectively, of the annelated ring was accomplished as shown in Figure 2.

As starting material 7-(2-bromoethyl)-8-bromotheophylline was used, the preparation of which had been described by Caccacae.[45] In our laboratory a modified procedure was developed using a two phase catalysis method (see Section 10). The other starting compounds, 7-(3-chloropropyl)-8-bromotheophylline and 7-(4-bromobutyl)-8-bromotheophylline, were obtained as previously described.[46,47] They were cyclized with amines

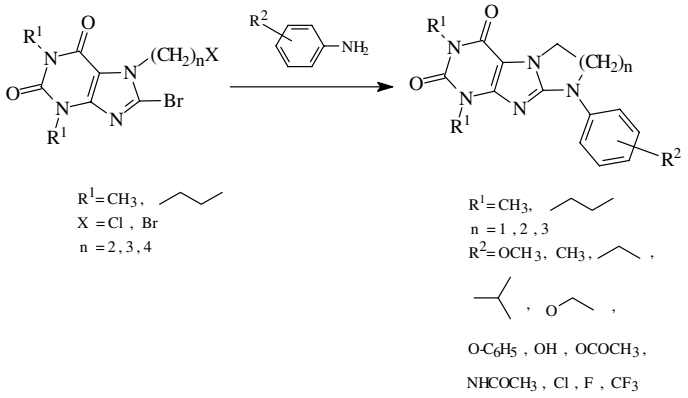

Figure 2. Synthesis of 1,3-dimethyl and 1,3-dipropylperhydro imidazo-, pyrimido-, and 1,3-diazepino[2,1-*f*]purinediones.

under various reaction conditions (excess of amine, solvent, and reaction time). The data are summarized in Table 1.

Unsubstituted compounds **1**, **11**, and **31** were synthesized with methods developed previously[48] and are now used in pharmacological tests for comparison of their biological activity with that of the substituted derivatives. The synthesis of compound **12** without substituent at the phenyl ring has been described previously.[49] 1,3-Dipropyl-7-(3-chloropropyl)-8-bromoxanthine was used as starting material for the synthesis of 1,3-dipropylderivatives (**39**, **40**).

The structures of the synthesized compounds were confirmed by UV, IR, and ^{1}H NMR spectra. UV spectra showed a bathochromic shift typical of 8-aminoxanthine derivatives of λ_{max} to about 300 nm.[50] The IR absorption bands were typical of xanthine derivatives[46,51] and in ^{1}H NMR adequate chemical shifts were recorded. Spectroscopic data are presented in Table 2.

3. X-ray structure analysis of compounds 37 and 40

To obtain representative structural data for molecular modeling studies, monocrystals suitable for X-ray structure analysis have been obtained for diazepinopurinedione **37** (purine 7) with $R^1 = CH_3$ and pyrimidopurinedione **40** with $R^1 = C_3H_7$.

The two molecules (Fig. 3) had a different third ring, which was 7- or 6-membered. Consequently significant difference in purine 7 and purine 6 tricycle planarity was observed (Fig. 4). As corresponding difference descriptor, total puckering amplitude Q[52,53] has been applied. The value for the 14-membered tricycle (group 7) in **37** is much higher (Q = 1.123(4) Å) than the one for the 13-membered cycle (group 6, subgroup +6) in **40** with Q = 0.506(6) Å. It has been evident consequence of various puckering amplitudes that Q for rings annelated to purine, equaled 0.664(4) Å for 7-membered in **37** and 0.452(6) Å for 6-membered one in **40**.

Beside ring dimensions, both molecules belong to two purine families with other aliphatic groups R^1. The CH_3 groups in **37** are in purine plane. But in **40**, both extended propyl chains—like propellers—are situated on opposite sides of the purine skeleton. Hence the last atoms of both chains (C1B for chain at N1 and C3B for chain at N3) are placed in a distance of—1.76(1) Å and 1.66(1) Å from the purine plane, respectively, for chains at N1 and N3.

Both molecules contain an aromatic substituent at N10 (and N9, respectively) in **37** and **40**. The phenyl ring is not coplanar with the tricycle (Table 3). That aromatic ring has no rotational restriction and its position in the molecule depends on the close crystal packing. It should be noted that sum of the valence angles around N9 and/or N10 atoms (Table 3) indicated a not exactly planar hybridization of those atoms in **37** and **40**.

In this study, intramolecular interactions are of particular interest (Fig. 3). Theoretically, for both molecules only weak H-bond with C(sp^3)–H as proton donors can be expected. However, only in the crystal of **37** have the weak H-bonds been observed (Table 3). The frequent H-bond nets in the crystal of **40** are dominated by the presence of water molecule (Table 3). Thus, beside the strong water–water bond, O1W–H2W···O4 interaction was present. It should be pointed out that this bond was formed with O4. Probably, the second oxygen O2 was shielded by two propyl chains. In the crystal of **37**, acidic carbon atoms are positioned as the exact neighborhood of electron-withdrawing nitrogens N5 and N10. In this crystal between C6–H6B···O4 an intermolecular H-bond was found. It is a consequence of C6 pushing out of the purine plane by 0.152(5) Å (the corresponding C6 in **40** deviates by 0.023(5) Å only). Also C9 has shown acidic character and C9–H9B···O2 interaction was identified. In those crystals, an additional weak H-bond of C15–H15···O2 has been observed (Table 3).

The X-ray structure analysis results constituted the starting point for subsequent modeling of the remaining molecules from this study. Moreover, interpretations of the crystal and molecular structures' architecture will be useful for the later pharmacophore model constructions.

4. Lipophilicity

Parameters of lipophilicity (log K_w) were determined experimentally by HPLC method on hydrocarbon silica (Inertsil) and immobilized artificial membrane (IAM) columns. Moreover log P values were calculated using the programs HyperChem[54] and CAChe;[55] log P and the distribution coefficient log D and pK_a values were calculated with PALLAS 3.1.[56] Calculated and experimental parameters describing physicochemical properties of the examined compounds are collected in Table 4.

5. Pharmacology

All compounds were tested in vitro in radioligand binding assays for affinity to A_1 and A_{2A} ARs in rat cortical membrane and rat striatal membrane preparations, respectively. Selected compounds were further tested for their affinity to human A_1, A_{2A}, A_{2B}, and A_3 receptors recombinantly expressed in CHO cells. As A_1 AR radioligand [^{3}H]2-chloro-N^6-cyclopentyladenosine ([^{3}H]CCPA)[57] was used and as A_{2A} radioligand [^{3}H]1-propargyl-3-(3-hydroxypropyl)-7-methyl-8-(*m*-methoxystyryl)xanthine ([^{3}H]MSX-2) was used.[58]. [^{3}H]4-(2-[7-amino-2-(2-furyl)-[1,2,4]-triazolo[2,3-*a*][1,3,5]-triazin-5-4-(amino)-ethyl)phenol ([^{3}H]ZM241385) was used as a radioligand in A_{2B} binding studies[59] and [^{3}H]2-phenyl-8-ethyl-4-methyl-(8*R*)-4,5,7,8-tetrahydro-1*H*-imidazo[2,1-*i*]purine-5-one ([^{3}H]PSB-11) was used as A_3 adenosine selective receptor ligand.[16]. The results are presented in Tables 5 and 6. The standard antagonists

Table 1. Physical data and reaction conditions of 8-, 9-, 10-aryloimidazo-, pyrimido-, and diazepino[2,1-*f*]purinediones

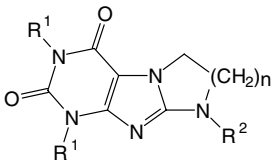

Compound	R^1	R^2	*n*	Molecular formula, M_w	Mp (°C)	Yield (%)	Reaction medium excess of amine	Reaction time	Crystal solvent	TLC R_f eluent
1	CH_3	H	1			Ref.46				
2	CH_3	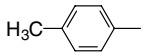	1	$C_{16}H_{17}N_5O_2$, 311.34	285–287	66	MeDigol 2	5	Methoxy-ethanol	0.74[a]
3	CH_3	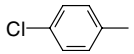	1	$C_{15}H_{14}N_5O_2Cl$, 331.76	308–309	71	MeDigol 2	5	DMF	0.74[b]
4	CH_3	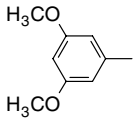	1	$C_{17}H_{19}N_5O_2$, 357.36	240–242	58	MeDigol 2	5	Methoxy-ethanol	0.85[c]
5	CH_3	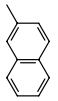	1	$C_{19}H_{17}N_5O_2$, 347.37	285–287	65	MeDigol 2	5	MeDigol	0.68[b]
6	CH_3	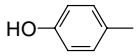	1	$C_{15}H_{15}N_5O_3$, 313.31	295–297	72	MeDigol 2	5	Methoxy-ethanol	0.83[a]
7	CH_3	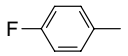	1	$C_{15}H_{14}N_5O_2F$, 315.3	301–302	62	MeDigol 2	5	MeDigol	0.77[d]
8	CH_3	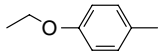	1	$C_{17}H_{19}N_6O_3$, 341.36	257–258	74	MeDigol 2	5	Methoxy-ethanol	0.74[b]
9	CH_3	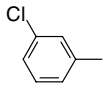	1	$C_{15}H_{14}N_5O_2Cl$, 333.76	252–253	50	MeDigol2	5	Methoxy-ethanol	0.69[b]

10	CH_3	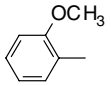	1	$C_{16}H_{17}N_5O_3$, 327.34	295–297	60	MeDigol2	5	Methoxy-ethanol	0.68[b]
11	CH_3	H	2			Ref. 46				
12	CH_3		2			Ref. 47				
13	CH_3	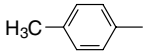	2	$C_{17}H_{19}N_5O_2$, 325.36	260–262	76	MeDigol2	5	Butanol	0.78[e]
14	CH_3	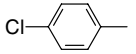	2	$C_{16}H_{16}N_5O_2Cl$, 345.79	285–287	67	MeDigol 2	5	Butanol	0.78[e]
15	CH_3		2	$C_{16}H_{16}N_5O_2Cl$, 345.79	264–267	64	23	10	Butanol	0.72[e]
16	CH_3	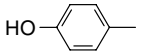	2	$C_{16}H_{17}N_5O_3$, 327.33	277–279	66	MeDigol 2	5	70% Propanol	0.75[e]
17	CH_3	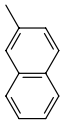	2	$C_{20}H_{19}N_5O_2$, 361.39	270–272	72	MeDigol 2	5	Butanol	0.79[e]
18	CH_3	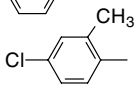	2	$C_{17}H_{18}N_5O_2Cl$, 359.81	239–241	35	MeDigol 2	10	Propanol	0.74[e]
19	CH_3	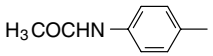	2	$C_{18}H_{20}N_6O_3$, 368.38	316–318	43	MeDigol 2	10	Ethanol	0.42[e]
20	CH_3	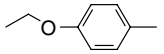	2	$C_{18}H_{21}N_5O_3$, 355.38	253–254	71	MeDigol 2	5	Butanol	0.73[e]
21	CH_3	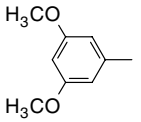	2	$C_{18}H_{21}N_5O_4$, 371.38	223–226	55	MeDigol 2	10	Butanol	0.73[e]
22	CH_3	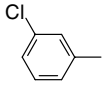	2	$C_{16}H_{16}N_5O_2Cl$, 345.78	270–271	62	MeDigol 2	5	Methoxyethanol	0.62[e]
23	CH_3	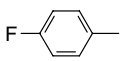	2	$C_{16}H_{16}N_5O_2F$, 329.33	288–290	74	MeDigol 2	6	MeDigol	0.75[f]

(*continued on next page*)

Table 1 (*continued*)

Compound	R^1	R^2	*n*	Molecular formula, M_w	Mp (°C)	Yield (%)	Reaction medium excess of amine	Reaction time	Crystal solvent	TLC R_f eluent
24	CH_3	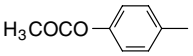	2	$C_{18}H_{19}N_5O_4$, 369.37	275–278	92	Acetyl anhydride	5	DMF	0.54[f]
25	CH_3	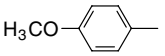	2	$C_{17}H_{19}N_5O_3$, 341.36	239–240	82	MeDigol 2	10	MeDigol	0.73[f]
26	CH_3	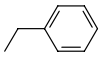	2	$C_{18}H_{21}N_5O_2$, 339.39	211–212	59	MeDigol 2	5	Butanol	0.49[f]
27	CH_3	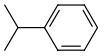	2	$C_{19}H_{23}N_5O_2$, 353.41	168–170	54	MeDigol 2	5	Ethanol	0.48[f]
28	CH_3	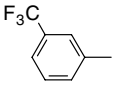	2	$C_{17}H_{16}N_5O_2F_3$, 379.34	210–212	70	EtDigol 2	10	Propanol	0.45[f]
29	CH_3	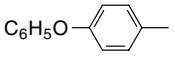	2	$C_{22}H_{21}N_5O_3$, 403.43	218–219	75	MeDigol 2	7	Methoxyethanol	
30	CH_3	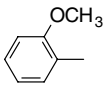	2	$C_{17}H_{19}N_5O_3$, 341.36		61	MeDigol2	10	1 propanol	0.72[d]
31	CH_3	H	3		Ref. 46					
32	CH_3	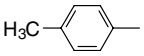	3	$C_{18}H_{21}N_5O_2$, 339.39	193–195	57	DMF 2	5	70% ethanol	0.72[f]
33	CH_3	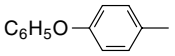	3	$C_{23}H_{23}N_5O_3$, 417.45	172–173	43	MeDigol 2	5	Methoxyethanol	0.71[f]

34	CH_3	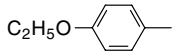	3	$C_{19}H_{23}N_5O_3$, 369.40	167–169	59	DMF 2	5	Propanol	0.65[f]
35	CH_3	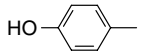	3	$C_{17}H_{19}N_5O_3$, 341.36	293–295	59	DMF 2	5	Methoxyethanol	0.40[f]
36	CH_3	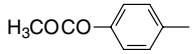	3	$C_{19}H_{21}N_5O_4$, 383.39	191–192	97	Acetyl anhydride	5	Propanol	0.63[f]
37	CH_3	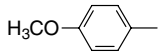	3	$C_{18}H_{21}N_5O_3$, 335.39	174–176	97	MeDigol 2	5	70% ethanol	0.60[f]
38	CH_3	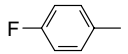	3	$C_{17}H_{18}N_5O_2F$ x H_2O, 361,37	194-196	73	DMF 2	5	Propanol	0.68[f]
39			2	$C_{24}H_{27}N_5O_2$, 417,49	174-176	81	DMF 2	5	Ethanol	0.68[f]
40		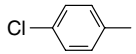	2	$C_{20}H_{24}N_5O_2Cl$, 401,89	146-148	83	DMF 2	5	Ethanol	0.74[f]

MeDigol, diethylene glycol monomethyl ether.
[a] Butanol/butyl acetate/$CHCl_3$—5:1:1+two drops of 25% NH_3 (aq).
[b] Butanol/butyl acetate/$CHCl_3$—5:1:1.
[c] Acetone/methanol/butyl acetate—1:1:1+two drops of 25% NH_3 (aq).
[d] Butanol/ethyl acetate/CH_2Cl_2—5:3:2.
[e] Butanol/butyl acetate/CH_2Cl_2—5:3:2.
[f] Benzene/acetone—7:3.

Table 2. Spectral data of 8-, 9-, 10- aryloimidazo-, pyrimidyno-, and diazepino[2,1-*f*]purinediones

Compound	UV λ_{max}, log ε	IR ν cm^{-1}	^{1}H NMR δ (ppm)
1	Ref. 46		
2	317.5, 4.36	1702-CO (pos. 2), 1650-CO (pos. 4)	$CDCl_3$, 2.35 (s, 3H, CH_3 phenyl), 3.41 (s, 3H, N_3CH_3), 3.63 (s, 3H, N_1CH_3), 4.43 (s, 4H, CH_2CH_2), 7.49 (d, 2H, J = 8.53 Hz, H2,6-phenyl), 7.24 (d, 2H, J = 7.18 Hz, H3,5-phenyl)
3	317.5, 4.30	1700-CO (pos. 2), 1660-CO (pos. 4)	$CDCl_3$, 3.42 (s, 3H, N_3CH_3), 3.62 (s, 3H, N_1CH_3), 4.46 (s, 4H, CH_2CH_2), 7.37 (d, 2H, J = 9.00 Hz, H2,6-phenyl), 7.57 (d, 2H, J = 9.02 Hz, H3,5-phenyl)
4	317.5, 4.38	1702-CO (pos. 2), 1660-CO (pos. 4)	$CDCl_3$, 3.40 (s, 3H, N_3CH_3), 3.58 (s, 3H, N_1CH_3), 3.83 (s, 6H, $2OCH_3$), 4.40 (s, 4H, CH_2CH_2), 6.19 (t, 1H, J = 2.08 Hz, H4-phenyl), 6.82 (d, 2H, J = 2.11 Hz, H2,6-phenyl)
5	319.5, 4.20	1705-CO (pos. 2), 1670-CO (pos. 4)	$CDCl_3$, 3.43 (s, 3H, N_3CH_3), 3.66 (s, 3H, N_1CH_3), 4.48 (s, 4H, CH_2CH_2), 7.40–7.91 (2m, 6H, naphthyl), 8.22 (dd, J = 2.31 Hz, 1H, H1-naphthyl)
6	318.5, 4.31	3200–3450-OH, 1702-CO (pos. 2), 1620-CO (pos. 4)	DMSO, 3.34 (s, 3H, N_3CH_3), 3.41 (s, 3H, N_1CH_3), 4.28–4.38 (m, 4H, CH_2CH_2), 6.81 (d, 2H, J = 8.9 Hz, 2H, H3,5-phenyl), 7.44 (d, J = 8.9 Hz, H2,6-phenyl), 9.2 (s, 1H, OH)
7	316.0, 4.16	1699-CO (pos. 2), 1651-CO (pos. 4)	$CDCl_3$, 3.43 (s, 3H, N_3CH_3), 3.63 (s, 3H, N_1CH_3), 4.47 (s, 4H, CH_2CH_2), 7.11–7.17 (m, 2H, H3,5-phenyl), 7.58–7.62 (m, 2H, H2,6-phenyl)
8	319.5, 4.33	1698-CO (pos. 2), 1640-CO (pos. 4)	$CDCl_3$, 1.42 (t, 3H, J = 6.57 Hz, OCH_2CH_3), 3.39 (s, 3H, N_3CH_3), 3.58 (s, 3H, N_1CH_3), 4.03 (q, 2H, J = 6.97 Hz, OCH_2CH_3), 4.38 (s, 4H, CH_2CH_2), 6.92–6.96 (m, 2H, H3,5-phenyl), 7.27–7.51 (m, 2H, H2,6-phenyl)
9	318.5, 4.39	1699-CO (pos. 2), 1649-CO (pos. 4)	DMSO, 3.17 (s, 3H, N_3CH_3), 3.42 (s, 3H, N_1CH_3), 4.28–4.48 (m, 4H, CH_2CH_2), 7.04 (d, 1H, J = 6.92 Hz, H6-phenyl), 7.39 (t, 1H, J = 8.21 Hz, H5-phenyl), 7.54 (d, J = 8.46 Hz, 1 H, H4-phenyl), 7.70 (s, 1H, H2-phenyl)
10	307.7, 4.31	1708-CO (pos. 2), 1659-CO (pos. 4)	$CDCl_3$, 3.40 (s, 3H, N_3CH_3), 3.51 (s, 3H, N_1CH_3), 3.87 (s, 3H, OCH_3), 4.32–4.46 (m, 4H, CH_2CH_2), 6.96–7.04 (m, 2H, H3,5-phenyl), 7.21–7.27 (m, 1H, H4-phenyl), 7.63 (d, J = 7.75 Hz, 1H, H6-phenyl)
11	Ref. 46		
12	Ref. 47		
13	306.5, 4.47	1701-CO (pos. 2), 1654-CO (pos. 4)	DMSO, 2.23–2.40 (m, 5H, CH_3 + $CH_2CH_2CH_2$), 3.36 (s, 3H, N_3CH_3), 3.42 (s, 3H, N_1CH_3), 3.83 (t, 2H, J = 6.05 Hz, N_9CH_2), 4.36 (t, 2H, J = 7.08 Hz, N_5CH_2), 7.35 (d, J = 7.52 Hz, 2H, H3,5-phenyl), 7.7 (d, 2H, J = 7.48 Hz, H2,6-phenyl)
14	306.0, 4.34	1703-CO (pos. 2), 1661-CO (pos. 4)	DMSO, 2.29–2.38 (m, 2H, $CH_2CH_2CH_2$), 3.37 (s, 3H, N_3CH_3), 3.45 (s, 3H, N_1CH_3), 3.83 (t, 2H, J = 7.28 Hz, N_9CH_2), 4.36 (t, 2H, J = 6.52 Hz, N_5CH_2), 7.27–7.45 (m, 4H, phenyl)
15	300.5, 4.42	1704-CO (pos. 2), 1653-CO (pos. 4)	$CDCl_3$, 2.28–2.37 (m, 2H, $CH_2CH_2CH_2$), 3.37 (s, 3H, N_3CH_3), 3.38 (s, 3H, N_1CH_3), 3.72–3.73 (m, 2H, N_9CH_2), 4.35–4.42 (m, 2H, N_5CH_2), 7.27–7.50 (m, 4H, phenyl)
16	304.0, 4.25	3579–3402-OH, 1695-CO (pos. 2), 1644-CO (pos. 4)	DMSO, 2.10–2.30 (m, 2H, $CH_2CH_2CH_2$), 3.12 (s, 3H, N_3CH_3), 3.18 (s, 3H, N_1CH_3), 3.65–3.70 (m, 2H, N_9CH_2), 4.13 (t, 2H, J = 5.6 Hz, N_5CH_2), 6.77 (d, 2H, J = 9.75 Hz, 2H, H3,5-phenyl), 7.24 (d, 2H, J = 8.75 Hz, H2,6-phenyl), 9.44 (s, 1H, OH)
17	310.0, 4.38	1658-CO (pos. 2), 1653-CO (pos. 4)	$CDCl_3$, 2.30–2.42 (m, 2H, $CH_2CH_2CH_2$), 3.39 (s, 3H, N_3CH_3), 3.45 (s, 3H, N_1CH_3), 3.97 (t, 2H, J = 5.59 Hz, N_9CH_2), 4.41 (t, 2H, J = 6.13 Hz, N_5CH_2), 7.44–7.80 (2m, 7H, naphthyl)

Table 2 (*continued*)

Compound	UV λ_{max}, log ε	IR ν cm^{-1}	^{1}H NMR δ (ppm)
18	301.0, 4.30	1699-CO (pos. 2), 1657-CO (pos. 4)	$CDCl_3$, 2.22 (s, 3H, CH_3), 2.26–2.38 (m, 2H, $CH_2CH_2CH_3$), 3.37 (s, 3H, N_3CH_3), 3.38 (s, 3H, N_1CH_3), 3.65 (s, 2H, N_9CH_2), 4.39 (s, 2H, N_5CH_2), 7.19–7.30 (m, 3H, phenyl)
19	308.0, 4.41	3297-NH, 1696-CO (pos. 2), 1659-CO (pos. 4)	DMSO, 2.04 (s, 3H, CH_3), 2.18–2.41 (m, 2H, $CH_2CH_2CH_2$), 3.19 (s, 3H, N_3CH_3), 3.27 (s, 3H, N_1CH_3), 3.77 (t, 2H, J = 5.28 Hz, N_9CH_2), 4.20 (t, 2H, J = 5.84 Hz, N_5CH_2), 7.41 (d, 2H, J = 8.97 Hz, H2,6-phenyl), 7.57 (d, 2H, J = 8.98 Hz, H3,5-phenyl), 9.96 (s, 1H, NH)
20	305.0, 4.29	1698-CO (pos. 2), 1660-CO (pos. 4)	$CDCl_3$, 1.42 (t, 3 H, J = 6.97 Hz, CH_3CH_2), 2.27–2.35 (m, 2H, $CH_2CH_2CH_2$), 3.37 (s, 3H, N_3CH_3), 3.43 (s, 3H, N_1CH_3), 3.79 (t, 2H, J = 5.57 Hz, N_9CH_2), 3.99–4.11 (q, 2H, J = 7.00 Hz, CH_2CH_3), 4.35 (t, 2H, J = 6.08 Hz, N_5CH_2), 6.89–6.95 (m, 2H, H3,5-phenyl), 7.28–7.36 (m, 2H, H2,6-phenyl)
21	304.0, 4.37	1687-CO (pos. 2), 1653-CO (pos. 4)	$CDCl_3$, 2.24–2.36 (m, 2H, $CH_2CH_2CH_2$), 3.37 (s, 3H, N_3CH_3), 3.47 (s, 3H, N_1CH_3), 3.80–3.87 (m, 8H, $2OCH_3$ + N_9CH_2), 4.35 (t, 2H, J = 6.08 Hz, N_5CH_2), 6.30 (t, 1H, J = 2.18 Hz, H4-phenyl), 6.70 (d, 2H, J = 2.19 Hz, H2,6-phenyl)
22	305.0, 4.34	1704-CO (pos. 2), 1652-CO (pos. 4)	$CDCl_3$, 2.28–2.37 (m, 2H, $CH_2CH_2CH_2$), 3.38 (s, 3H, N_3CH_3), 3.49 (s, 3H, N_1CH_3), 3.85 (t, 2H, J = 5.63 Hz, N_9CH_2), 4.37 (t, 2H, J = 6.26 Hz, N_5CH_2), (m, 4H, phenyl)
23	303.0, 4.31	1703-CO (pos. 2), 1664-CO (pos. 4)	$CDCl_3$, 2.28–2.36 (m, 2H, $CH_2CH_2CH_2$), 3.38 (s, 3H, N_3CH_3), 3.44 (s, 2H, N_1CH_3), 3.82 (t, 2H, J = 5.64 Hz, N_9CH_2), 4.37 (t, 2H, J = 6.16 Hz, N_5CH_2), 7.04–7.12 (m, 2H, H3,5-phenyl), 7.23–7.44 (m, 2H, H2,6-phenyl)
24	305.0, 4.32	1701-CO (pos. 2), 1664-CO (pos. 4)	$CDCl_3$, 2.32–2.42 (m, 5H, $COCH_3$ + $CH_2CH_2CH_2$), 3.39 (s, 3H, N_3CH_3), 3.46 (s, 3H, N_1CH_3), 3.85 (t, 2H, J = 5.57 Hz, N_9CH_2), 4.37 (t, 2H, J = 6.09 Hz, N_5CH_2), 7.09–7.13 (m, 2H, H3,5-phenyl), 7.47–7,54 (m, 2H, H2,6-phenyl)
25	303.0, 4.33	1703-CO (pos. 2), 1661-CO (pos. 4)	$CDCl_3$, 2.26–2.34 (m, 2H, $CH_2CH_2CH_2$), 3.38 (s, 3H, N_3CH_3), 3.44 (s, 3H, N_1CH_3), 3.79 (t, 2H, J = 5.56 Hz, N_9CH_2), 3.83 (s, 3H, OCH_3), 6.90–6.95 (m, 2H, H3,5-phenyl), 7.26–7.36 (m, 2H, H2,6-phenyl)
26	306.0, 4.35	1698-CO (pos. 2), 1653-CO (pos. 4)	$CDCl_3$, 1.25 (t, 3H, J = 7.56 Hz, CH_2CH_3), 2.25–2.33 (m, 2H, $CH_2CH_2CH_2$), 2.65 (q, 2H, J = 7.55 Hz, CH_2CH_3), 3.36 (s, 3H, N_3CH_3), 3.44 (s, 3H, N_1CH_3), 3.83 (t, 2H, J = 5.49 Hz, N_9CH_2), 4.34 (t, 2H, J = 6.04 Hz, N_5CH_2), 7.21 (d, 2H, J = 8.5 Hz, H2,6-phenyl), 7.36 (d, 2H, J = 8.5 Hz, H3,5-phenyl)
27	303.0, 4.34	1703-CO (pos. 2), 1658-CO (pos. 4)	$CDCl_3$, 1.26 (d, 6H, J = 6.87 Hz, $2CH_3$), 2.20–2.38 (m, 2H, $CH_2CH_2CH_2$), 2.80–3.00 (m, 1H, $CH(CH_3)_2$), 3.37 (s, 3H, N_3CH_3), 3.45 (s, 3H, N_1CH_3), 3.83 (t, 2H, N_9CH_2), 4.35 (t, 2H, N_5CH_2), 7.23 (d, 2H, J = 8.5 Hz, H3,5-phenyl), 7.37 (d, 2H, J = 8.5 Hz, H2,6-phenyl)
28	305.0, 4.30	1698-CO (pos. 2), 1661-CO (pos. 4)	$CDCl_3$, 2.16–2.39 (m, 2H, $CH_2CH_2CH_2$), 3.38 (s, 3H, N_3CH_3), 3.46 (s, 3H, N_1CH_3), 3.90 (t, 2H, J = 5.49 Hz, N_9CH_2), 4.39 (t, 2H, J = 6.04 Hz, N_5CH_2), 7.41 (d, 1H, J = 7.69 Hz, H6-phenyl), 7.50 (t, 1H, J = 8.14 Hz, H5-phenyl), 7.70 (d, 1H, J = 7.97 Hz, H4-phenyl), 7.81 (s, 1H,H2-phenyl)
29	308.0, 4.34	1708-CO (pos. 2), 1651-CO (pos. 4)	$CDCl_3$, 2.27–2.33 (m, 2H, $CH_2CH_2CH_2$), 3.36 (s, 3H, N_3CH_3), 3.44 (s, 3H, N_1CH_3), 3.83 (t, 2H, J = 5.56 Hz, N_9CH_2), 4.35 (t, 2H, J = 6.07 Hz, N_5CH_2), 6.00–7.14 (m, 5H, OC_6H_5), 7.27–7.44 (m, 4H, phenyl)

(*continued on next page*)

Table 2 (*continued*)

Compound	UV λ_{max}, log ε	IR ν cm^{-1}	^{1}H NMR δ (ppm)
30	302.0, 4.32	1695-CO (pos. 2), 1661-CO (pos. 4)	$CDCl_3$, 2.22–2.33 (m, 2H, $CH_2CH_2CH_2$), 3.37 (s, 6H, N_3CH_3 + N_1CH_3), 3.68 (t, 2H, J = 5.88 Hz, N_9CH_2), 3.82 (s, 3H, OCH_3), 4.36 (t, 2H, J = 6.05 Hz, N_5CH_2), 6.96–7.05 (m, 2H, H4,5-phenyl), 7.27–7.37 (m, 2H, H3,6-phenyl)
31	Ref. 46		
32	308.0, 4.38	1701-CO (pos. 2), 1646-CO (pos. 4)	$CDCl_3$, 1.96 (s, 4H, $(CH_2)_2$), 2.32 (s, 3H, CH_3), 3.39 (s, 3H, N_3CH_3), 3.44 (s, 3H, N_1CH_3), 3.76 (br s, 2H, $N_{10}CH_2$), 4.48 (br s, 2H, N_5CH_2), 7.01 (d, 2H, J = 6.5 Hz, H3,5-phenyl), 7.11 (d, 2H, J = 6.0 Hz, H2,6-phenyl)
33	307.0, 4.40	1700-CO (pos. 2), 1644-CO (pos. 4)	$CDCl_3$, 1.98 (br s, 4H, $(CH_2)_2$), 3.40 (s, 3H, N_3CH_3), 3.46 (s, 3H, N_1CH_3), 3.77 (br s, 2H, $N_{10}CH_2$), 4.32 (br s, 2H, N_5CH_2), 6.96–7.03 (m, 2H, H3,5-phenyl), 7.10–7.16 (m, 2H, H2,6-phenyl), 7.26–7.37 (m, 5H, OC_6H_5)
34	304.0, 4.40	1702-CO (pos. 2), 1644-CO (pos. 4)	$CDCl_3$, 1.41 (t, 3H, J = 6.9 Hz, CH_2CH_3), 1.97–1.98 (br s, 4H, $(CH_2)_2$), 3.38 (s, 3H, N_3CH_3), 3.41 (s, 3H, N_1CH_3), 3.73 (br s, 3H, $N_{10}CH_2$), 3.82 (q, 2H, J = 6.9 Hz, CH_2CH_3), 4.48 (br s, 2H, N_5CH_2), 6.84–6.88 (m, 2H, H3,5-phenyl), 7.09–7.10 (m, 2H, H2,6-phenyl)
35	307.0, 4.37	3414 -OH, 1699-CO (pos. 2), 1647-CO (pos. 4)	$CDCl_3$, 1.96 (s, 4H, $(CH_2)_2$), 3.20 (s, 3H, N_3CH_3), 3.36 (s, 3H, N_1CH_3), 3.69 (br s, 2H, $N_{10}CH_2$), 4.35 (br s, 2H, N_5CH_2), 6.72 (d, 2H, J = 6.8 Hz, H3,5-phenyl), 7.07 (d, 2H, J = 6.8 Hz, H2,6-phenyl), 9.34 (s, 1H, OH)
36	307.0, 4.39	1764-$OCOCH_3$, 1702-CO (pos. 2), 1644-CO (pos. 4)	DMSO, 1.95 (s, 4H, $(CH_2)_2$), 2.27 (s, 3H, $COCH_3$), 3.38 (s, 3H, N_3CH_3), 3.44 (s, 3H, N_1CH_3), 3.75 (br s, 2H, $N_{10}CH_2$), 4.43 (br s, 2H, N_5CH_2), 6.99 (d, 2H, J = 8.9 Hz, H3,5-phenyl), 7.15 (d, 2H, J = 8.5 Hz, H2,6-phenyl)
37	309.0, 4.40	1700-CO (pos. 2), 1644-CO (pos. 4)	$CDCl_3$, 1.96–1.99 (m, 4H, $(CH_2)_2$), 3.39 (s, 3H, N_3CH_3), 3.42 (s, 3H, N_1CH_3), 3,73 (t, 2H, J = 6.9 Hz, $N_{10}CH_2$), 3,81 (s, 3H, OCH_3), 4.50 (t, 2H, J = 5.5 Hz, N_5CH_2), 6.84–6.91 (m, 2H, H3,5-phenyl), 7.1–7.16 (m, 2H, H2,6-phenyl)
38	303.0, 4.28	3433-OH, 1701-CO (pos. 2), 1646-CO (pos. 4)	$CDCl_3$, 1.81–1.98 (m, 4H, $(CH_2)_2$), 3.39 (s, 3H, N_3CH_3), 3,44 (s, 3H, N_1CH_3), 3,75 (t, 3H, J = 6.0 Hz, $N_{10}CH_2$), 4.51 (t, 2H, J = 6.5 Hz, N_5CH_2), 6.93–7.07 (m, 2H, H3,5-phenyl), 7.1–7.18 (m, 2H, H2,6-phenyl)
39	311.0, 4.40	1693-CO (pos. 2), 1651-CO (pos. 4)	$CDCl_3$, 0.90–0.99 (m, 6H, $2CH_3CH_2CH_2$), 1.63–1.78 (m, 4H, $2CH_3CH_2CH_2$), 2.32–2.40 (m, 2H, $N_5CH_2CH_2CH_2N_9$), 3.92–3.99 (m, 6H, $2CH_2CH_2CH_3$ + N_9CH_2), 4.41 (t, 2H, J = 6.05 Hz, N_5CH_2), 7.42–7.86 (m, 7H, naphthyl)
40	308.5, 4.38	1696-CO (pos. 2), 1655-CO (pos. 4)	$CDCl_3$, 0.89–0.97 (m, 6H, $2CH_3CH_2CH_2$), 1.60–1.79 (m, 4H, $2CH_3CH_2CH_2$), 2.27–2.35 (m, 2H, $N_5CH_2CH_2CH_2N_9$), 3.82 (t, 2H, N_9CH_2), 3.81–3.96 (m, 4H, $2CH_2CH_2CH_3$), 4.36 (t, 2H, J = 6.05 Hz, N_5CH_2), 7.32–7.43 (m, 4H, phenyl)

caffeine (non-selective) and **KW-6002** (A_{2A}-selective) were included for comparison. Sodium chloride shift experiments[60] were performed for one of the most potent and A_{2A}-selective compounds of the present series in order to investigate whether the *N*-phenyl-substituted tricyclic xanthine derivatives are antagonists or agonists at the A_{2A} ARs (see Fig. 5).

Compounds were evaluated in vivo as anticonvulsants by the Antiepileptic Drug Development Program (ADD) of the National Institute of Neurological Disorders and Stroke NINDS according to the Antiepileptic Screening Project (ASP).[62–64] Phase I of the evaluation included three tests: maximal electroshock (MES), subcutaneous pentylenetetrazol (scMet), and the rotorod test for neurological toxicity (TOX) performed on mice. The MES assay has predictive value for agents of therapeutic potential in the management of grand mal epilepsy, whereas the scMet test is for those likely to be effective against petit mal.[62–64] For some compounds,

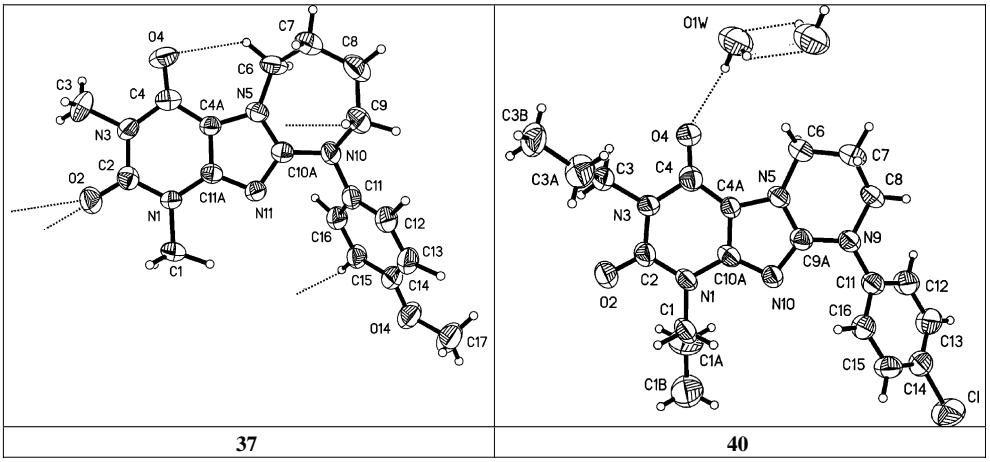

Figure 3. ORTEP drawing of **37** and **40** with H-bonds arrangement.

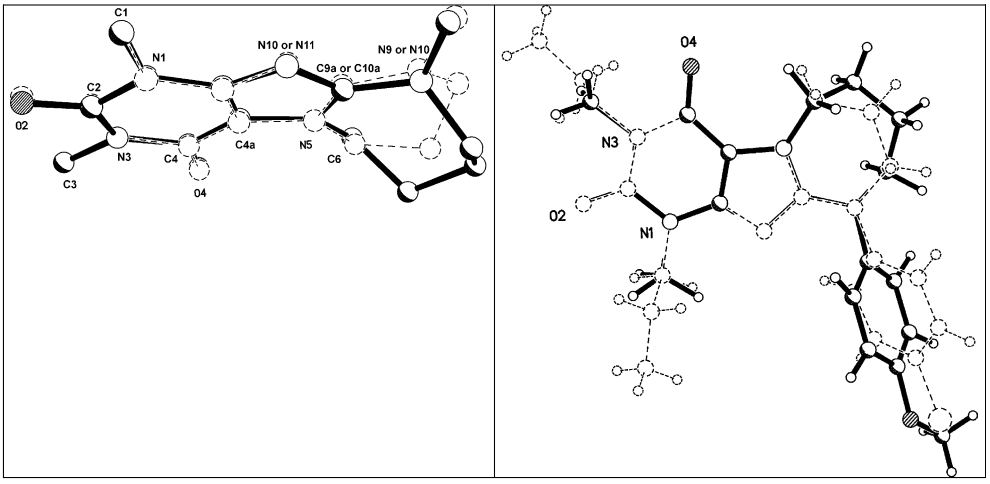

Figure 4. Superimposition of tricycle moieties in **37** (solid lines) and in **40** (dotted lines).

Table 3. Selected geometrical data from **37** and **40** molecules

(a) Molecules geometry

	37	**40**
Dihedral angle tricycle/phenyl (°)	74.9(4)	99.0(4)
C9–N10 (C8–N9)–C11–C12 (°)	66.7(4)	56.4(4)
$\sum$ angles at N10 (N9) (°)	356.2	358.1
Total puckering amplitude for tricycle Q (Å)	1.123(4)	0.506(6)

(b) H-bonds in the crystals

	D–H···A	Sym. code	D–H (Å)	H···A (Å)	D···A (Å)	D–H···A (°)
37	C5—H5B··· O4		1.03	2.42	3.171(5)	129
	C8–H8B··· O2	$-x, 1-y, -z$	1.16	2.41	3.377(5)	139
	C15–H15 ··· O2	$1/2-x, 1/2-y, -z$	1.09	2.17	3.153(4)	150
40	O1W–H1W···O1W	$-x, 1-y, 1-z$	0.84	2.16	2.782(7)	131
	O1W–H2W···O4		0.91	2.17	2.938(7)	142

namely **14**, **15**, **17**, and **18**, the TTE (threshold tonic extension) test was performed. The TTE test is clinically nonselective electroconvulsive seizure model similar to the MES screen but used at a lower level of electric current. It identifies compounds that raise the seizure threshold as well as those that prevent seizure spread.[62–64] The results of phase I tests are summarized in Table 7.

Compound **17** was also administered orally to rats and examined in the MES and TOX tests The results are presented in Table 8.

Table 4. Calculated and experimental parameters of lipophilicity of 8-, 9-, 10- aryloimidazo-, pyrimidyno-, and diazepino[2,1-*f*]purinediones

Compound	pK_a PALLAS	log *P* HyperChem	log *P* CAChe	log *P* PALLAS	log *D* (pH 7.0) PALLAS	log *D* (pH 7.4) PALLAS	log K_w IAM	log K_w Inertsil
1	7.41	−0.73	−0.50	−1.01	−1.55	−1.31	0.007	0.337
2	7.27	1.81	1.89	1.41	0.96	1.17	1.649	2.459
3	6.60	1.86	1.94	1.70	1.56	1.64	1.829	2.698
4	6.83	0.84	0.92	1.08	0.86	0.97	1.603	2.345
5	7.13	2.34	2.43	2.20	1.83	2.01	2.054	2.858
6	6.97	1.06	1.14	0.43	0.14	0.28	1.222	0.815
7	6.64	1.48	1.56	1.13	0.97	1.06	1.617	2.188
8	7.02	1.43	1.51	1.39	1.09	1.24	1.609	2.442
9	6.60	1.86	1.94	1.76	1.62	1.70		
10	7.01	1.09	1.17	0.94	0.64	0.79	1.001	1.649
11	7.24	−0.67	0.08	−0.50	−0.93	−0.72	0.375	0.251
12	7.04	1.39	2.01	1.49	1.17	1.33	0.714	1.333
13	7.13	1.86	2.47	1.92	1.55	1.73	1.356	2.222
14	6.46	1.91	2.53	2.21	2.10	2.17	1.408	1.945
15	6.46	1.91	2.53	2.20	2.09	2.15	1.177	1.435
16	6.84	1.11	1.72	0.94	0.71	0.83	0.647	0.717
17	7.00	2.40	3.52	2.71	2.41	2.56	1.989	2.177
18	6.55	2.38	2.99	2.80	2.67	2.74	1.573	1.975
19	7.10	0.24	0.86	0.48	0.13	0.31	0.456	0.610
20	6.88	1.48	2.10	1.90	1.66	1.79	1.355	2.238
21	6.69	0.89	1.50	1.59	1.42	1.51	1.210	1.683
22	6.46	1.91	2.53	2.27	2.16	2.22	1.793	2.466
23	6.50	1.53	2.15	1.64	1.52	1.59	1.217	1.471
24	6.43	0.89	1.51	1.03	0.93	0.99	0.816	1.297
25	6.87	1.14	1.75	1.44	1.21	1.33	1.223	1.333
26	7.15	2.26	2.87	2.46	2.08	2.27	1.595	2.160
27	7.15	2.59	3.20	2.78	2.40	2.59	1.928	2.474
28	6.2	2.28	2.89	2.70	2.62	2.67	1.879	2.244
29	6.65	2.82	3.44	3.17	3.01	3.10		
30	6.87	1.14	1.75	1.45	1.21	1.31		
31	8.09	1.85	0.53	0.01	−1.11	−0.75	0.237	0.420
32	7.99	2.31	2.93	2.43	1.41	1.75	1.367	2.018
33	7.50	3.27	3.89	3.68	3.07	3.33	2.333	3.728
34	7.73	1.94	2.55	2.41	1.61	1.92	1.234	2.039
35	7.69	1.56	2.17	1.45	0.67	0.96	0.894	1.235
36	7.28	1.34	1.96	1.54	1.08	1.30	1.029	2.016
37	7.72	1.59	2.21	1.95	1.16	1.46		
38	7.36	1.98	2.60	2.15	1.64	1.79	1.094	1.769
39	6.95	4.02	4.63	4.65	4.37	4.52	2.898	3.365
40	6.40	3.53	4.15	4.16	4.06	4.11	2.651	3.116

6. Results of biological studies

6.1. In vitro tests

The results of the binding assays toward rat adenosine A_1 and A_{2A} receptors (Table 5) exhibited that 1,3-dimethyl-arylimidazo-, pyrimido-, and 1,3-diazepinopurinediones showed affinity preferably for A_{2A} receptors. The size of annelated ring had a profound effect on the affinity. The graph shown in Figure 6 illustrates the A_{2A} affinity for selected groups of compounds (K_i < 25 μM). As it is visible (Fig. 6), a pyrimidine ring was beneficial for high A_{2A} affinity. Decrease to 5-membered (compounds **1**–**10**) or enlargement to 7-membered rings (compounds **31**–**38**) led to the reduction in adenosine receptor affinity in the following order: pyrimidine > diazepine > imidazole. Introduction of an aryl ring to the annelated system caused an increase in the affinity in comparison with unsubstituted derivatives (**1**, **11**, **31**). Among unsubstituted compounds, only pyrimidine derivative (**11**) exhibited affinity to A_{2A} adenosine receptor in the low micromolar range. Introduction of a substituent in the p-position of the phenyl ring had profitable effect on affinity (**14**, **16**, **23**, **25**—pyrimidine group; **35**, **37**—diazepines) and even in imidazopurinediones (**6** and **7**). The rank order of potency according to the nature of the substituent was as follows:

F > Cl > OCH_3 > OH > ethyl > isopropyl > $OCOCH_3$ > $NHCOCH_3$ > OC_2H_5. Compounds with a *p*-OH even in imidazo (**6**) and diazepine (**35**) derivatives had good affinity. Acetylation of OH decreased affinity: compare hydroxyl compounds **16** (K_i = 1.62 μM) and **35** (K_i = 1.60 μM) with their acetyl derivatives **24** (K_i = 3.12 μM) and **36** (K_i > 25 μM).

The best A_{2A} ligand was compound **23** with p-fluoro substituent (K_i = 0.147 μM and 170-fold A_{2A} selectivity). Submicromolar affinity was also shown by the

Table 5. Adenosine A_1 and A_{2A} receptor affinities of N-aryl-substituted imidazo-, pyrimido- and diazepino[2,1-*f*]purinediones in comparison with the standard compounds caffeine and **KW-6002**

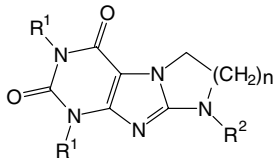

Compound	R^1	R^2	*n*	A_1[a] versus [^{3}H]CCPA		A_{2A}[a] versus [^{3}H]MSX-2		A_{2A} selectivity A_1/A_{2A}
				% inhibition ± SEM at 25 μM[b]	K_i ± SEM (μM)	% inhibition ± SEM at 25 μM[b]	K_i ± SEM (μM)	
Caffeine	—	**I**: R = CH_3 (fig. 1)	—	n.d.[c]	18.8 ± 5.6	n.d.[c]	32.5 ± 8.0	—
KW-6002	—	Figure 1	—	n.d.[c]	0.230 ± 0.030	n.d.[c]	0.00515 ± 0.00025	
Imidazo[2,1-f]purinediones								
1	CH_3	H	1	12 ± 4	>25	45 ± 2	⩾25	—
2	CH_3	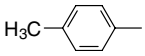	1	0 (2.5 μM)	⩾2.5	0 (2.5 μM)	⩾2.5	—
3	CH_3	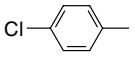	1	3 ± 3 (2.5 μM)	⩾2.5	58 ± 6 (2.5 μM)		
4	CH_3	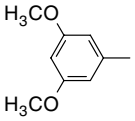	1	0 (2.5 μM)	⩾2.5	11 ± 0 (2.5 μM)	>2.5	—
5	CH_3	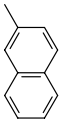	1	0	⩾25	0	⩾25	—
6	CH_3	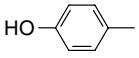	1	12 ± 4	>25	73 ± 3	2.33 ± 0.15	>11
7	CH_3	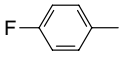	1	19 ± 4	>25	55 ± 3	5.25 ± 1.06	>5
8	CH_3	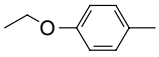	1	5 ± 4 (2.5 μM)	>2.5	31 ± 8 (2.5 μM)	>2.5	—
9	CH_3	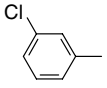	1	55 ± 4 (10 μM)	1.28 ± 0.38	57 ± 4	5.74 ± 1.23	4.5
10	CH_3	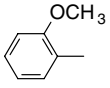	1	49 ± 4 (10 μM)	1.67 ± 0.24	59 ± 1 (10 μM)	6.05 ± 0.38	0.3
Pyrimido[2,1-f]purinediones								
11	CH_3	H	2	30 ± 3	>25	84 ± 7	5.22 ± 0.90	>4.8
12	CH_3		2	20 ± 1	>25	78 ± 4	3.52 ± 1.20	>7
13	CH_3	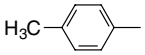	2	3 ± 1	>25	16 ± 6	>25	—
14	CH_3	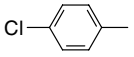	2	47 ± 1	>25	88 ± 5	1.12 ± 0.43	>22
15	CH_3		2	37 ± 2	>25	94 ± 3	2.35 ± 0.62	>11

(*continued on next page*)

Table 5 (*continued*)

Compound	R^1	R^2	*n*	A_1[a] versus [^{3}H]CCPA		A_{2A}[a] versus [^{3}H]MSX-2		A_{2A} selectivity A_1/A_{2A}
				% inhibition ± SEM at 25 μM[b]	K_i ± SEM (μM)	% inhibition ± SEM at 25 μM[b]	K_i ± SEM (μM)	
16	CH_3	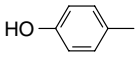	2	42[d]	35.0 ± 2.0	96[d]	1.62 ± 0.31	22
17	CH_3	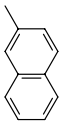	2	30 ± 1	⩾25	99[d]	0.219 ± 0.007	⩾114
18	CH_3	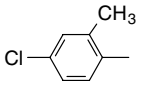	2	23 ± 7	>25	89 ± 7	2.94 ± 0.13	>9
19	CH_3	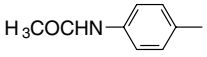	2	38 ± 2	⩾25	88 ± 4	3.82 ± 0.15	⩾7
20	CH_3	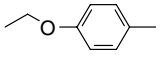	2	0	⩾25	32 ± 3	>25	—
21	CH_3	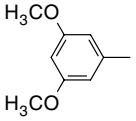	2	52[d]	8.01 ± 0.84	94[d]	2.84 ± 0.17	2.8
22	CH_3	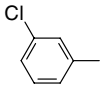	2	21 ± 11	>25	18 ± 8	>25	
23	CH_3	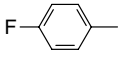	2	11 ± 1	>25	75 ± 8	0.147 ± 0.020	>170
24	CH_3	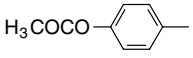	2	23 ± 1	>25	85 ± 4	3.12 ± 1.1	>8
25	CH_3	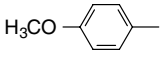	2	29 ± 3	>25	94 ± 6	0.998 ± 0.7	>25
26	CH_3	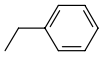	2	39 ± 3	⩾25	90 ± 10	1.46 ± 0.24	⩾17
27	CH_3	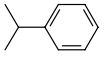	2	35 ± 2	>25	91 ± 7	1.75 ± 0.02	>14
28	CH_3	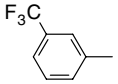	2	50 ± 4	>25	76 ± 1	2.66 ± 0.76	>9
29	CH_3	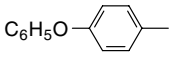	2	15 ± 10 (10 μM)	19.1 ± 0.3	102 ± 0 (10 μM)	0.299 ± 0.074	64
30	CH_3	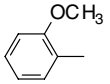	2	17 ± 5	>25	45 ± 6	⩾25	—
Diazepino[2,1-f]purinediones								
31	CH_3	H	3	33 ± 3	⩾25	38 ± 9	⩾25	—
32	CH_3	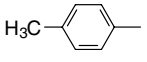	3	40 ± 2	⩾25	80 ± 3	4.16 ± .48	⩾6
33	CH_3	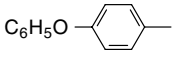	3	7 ± 2	>25	44 ± 1	⩾25	—

Table 5 (*continued*)

Compound	R^1	R^2	*n*	A_1[a] versus [^{3}H]CCPA		A_{2A}[a] versus [^{3}H]MSX-2		A_{2A} selectivity A_1/A_{2A}
				% inhibition ± SEM at 25 μM[b]	K_i ± SEM (μM)	% inhibition ± SEM at 25 μM[b]	K_i ± SEM (μM)	
34	CH_3	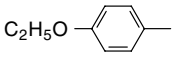	3	25 ± 4	>25	80 ± 5	6.23 ± 2.18	>4
35	CH_3	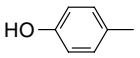	3	30 ± 5	>25	59 ± 8	1.60 ± 0.02	>6
36	CH_3	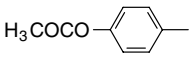	3	15 ± 6	>25	55 ± 7	22.3 ± 1.9	—
37	CH_3	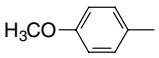	3	26 ± 1	>25	83 ± 4	3.29 ± 0.40	>8
38	CH_3	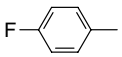	3	28 ± 3	>25	84 ± 2	8.72 ± 2.62	>3
39		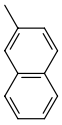	2	62 ± 4	1.29 ± 0.32	97 ± 1	0.398 ± 0.111	3.2
40		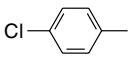	2	85 ± 2	0.36 ± 0.06	85 ± 1	0.376 ± 0.095	1

[a] Results are from at least three independent experiments performed in triplicate.
[b] In some cases the highest concentration used was 2.5 or 10 μM (as indicated) due to limited solubility of the compound.
[c] n.d., not determined.

2-naphthyl derivative **17** (K_i = 0.219 μM and 114-fold A_{2A} selectivity). Replacement of the methyl substituents in the purinedione system by propyl (compounds **39** and **40**) improved affinity to both receptor subtypes but reduced selectivity (see Table 5). Affinity to the human A_{2A} receptor of compound **23** was found to be somewhat lower as compared to the rat receptor (see Table 6). Some compounds, namely **11**, **17**, and **23**, showed affinity to the human A_{2B} receptor inhibiting radioligand binding by about 50% at the concentration of 10 μM but significantly lower affinity to the human A_1 receptor (about 10–20% inhibition at 10 μM). The affinity to the human A_3 receptor of the dipropyl derivatives (**39** and **40**) was very weak (see Table 6). The most potent A_{2A}-selective ligand of the present series was investigated for its functional properties using a sodium chloride shift assay. while the curve for the agonist NECA was significantly shifted to the right in the presence of 100 mM of sodium chloride, the curve for **17** was slightly, but not significantly, shifted to the left. This clearly indicated that **17** acts as an antagonist at A_{2A} receptors (Fig. 5).

6.2. In vivo tests

Unsubstituted imidazo-, pyrimido-, and diazepinopurinediones did not show protective activity in both electric and chemical seizures (Table 7). Introduction of an aryl substituent at the nitrogen atom of the annelated ring resulted in anticonvulsant activity. The size of the annelated ring, the character and the position of the substituent at the aryl ring seemed to have a significant influence on the profile and strength of the anticonvulsant activity. Among the imidazo- and diazepino-purinediones, only compounds **8**, **9**, **35**, and **37** showed anticonvulsant activity in chemical seizures at the high dose of 300 mg/kg. Among pyrimidopurinediones significantly more compounds showed protective activity in both tests (compounds **13**, **14**, **16**, and **20**) or scMet test (compounds **23**, **26**, **28**, and **30**). Para-substitution and electron-withdrawing substituents (CH_3, Cl, OH, F, and C_2H_5) were beneficial for anticonvulsant activity. Practically all investigated substances showed neurotoxicity in short (0.5 h) and long (4 h) time tests. All TTE tests were negative. Only compound **17** (completely inactive in MES and scMet tests) showed activity in TTE test after 0.25, 1, 2, and 4 h (Table 8). Compound **17** was also administered orally to rats showing protection in MES test in 0.25, 1, 2, and 4 h time at a dose of 30 mg/kg with no symptoms of neurotoxicity.

Contrary to our previous work[44] on oxazolo[2,3-*f*]purinediones a coincidence of adenosine A_{2A} affinity and anticonvulsant activity of pyrimido[2,1-*f*]purinediones was observed. Very recent work[65] discussing relationship between anticonvulsant effects and adenosine receptor activity indicated proconvulsant effects of adenosine antagonists especially for xanthines which are able to cross blood–brain-barrier. Moreover, anticonvulsant

Table 6. Affinities of selected compounds and standard antagonists at human adenosine A_1, A_{2A}, A_{2B} and A_3 receptors recombinantly expressed in Chinese hamster ovary cells

Compound	A_1	A_{2A}	A_{2B}	A_3
	$K_i \pm$ SEM[a] (μM) versus [^{3}H]CCPA	$K_i \pm$ SEM[a] (μM) versus [^{3}H]MSX-2	$K_i \pm$ SEM[b] (μM) versus [^{3}H]ZM-241385	$K_i \pm$ SEM[b] (μM) versus [^{3}H]PSB-11
Caffeine	44.9 ± 6.2	23.4 ± 7.1	20.5 ± 2.2[c]	n.d.[e]
KW-6002	2.07 ± 0.43	0.0908 ± 0.0228	n.d.[e]	4.47 ± 4.06
11	8.88 ± 0.72	19.3 ± 0.8	~10 (49%)[d]	>10 (10%)[d]
17	26.8 ± 1.2	2.87 ± 1.0	~10 (61%)[d]	>10 (10%)[d]
23	16.7 ± 1.7	1.88 ± 0.93	~10 (47%)[d]	>10 (19%)[d]
39	15.2 ± 2.4	1.39 ± 0.34	n.d.[e]	>10 (11%)[d]
40	12.2 ± 0.5	1.68 ± 0.34	n.d.[e]	>10 (7%)[d]

[a] Determined in at least three separate experiments each in triplicate.
[b] Determined in at least two separate experiments each in triplicate.
[c] Versus [^{3}H]PSB-298 as A_{2B} radioligand.[61]
[d] Percent inhibition of radioligand binding at 10 μM.
[e] n.d., not determined.

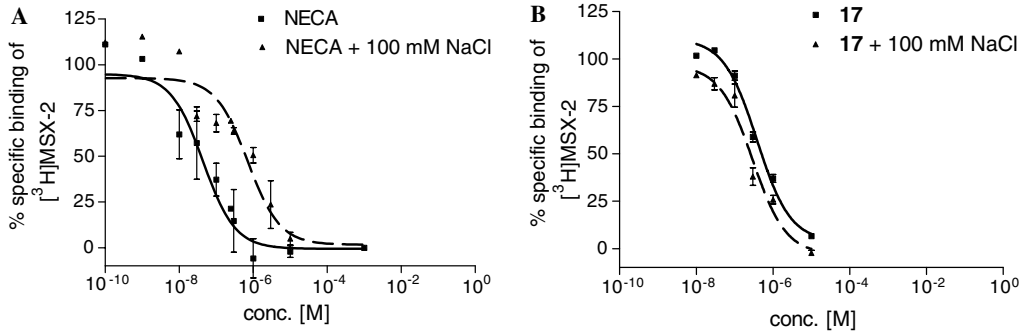

Figure 5. Radioligand binding curves of the agonist *N*-ethylcarboxamidoadenosine (NECA) and pyrimidopurine derivative **17** at adenosine A_{2A} receptors of rat brain striatal membrane preparations in the absence and in the presence of NaCl (100 mM).

effects were associated with adenosine A_1 receptor agonists, but not with A_{2A} agonists or antagonists. Taking the above into account, the displayed activity of the compounds investigated in this study and their correlation is not clear.

7. Physicochemical properties and SRRs studies

Experimental descriptors of lipophilicity ($\log K_w$) were determined for 36 compounds by HPLC on hydrocarbon silica (Inertstil) and additionally by immobilized artificial membrane (IAM) columns (four compounds, i.e., **9**, **29**, **30**, and **37**, devoid of ARs affinity, were not considered). Independently, theoretical descriptors of lipophilicity have been calculated for all compounds by means of the programs HyperChem, CAChe, and PALLAS (Table 4). Having the numbers of lipophilicity descriptors, it was interesting to compare calculated with experimental ones. First the relation between both experimental values was inspected. It was established that the experimental values of $\log K_w$s (Inertsil and IAM) were not higher than 3.8 and the values of $\log K_w$ (Inertsil) were generally higher than $\log K_w$ (IAM) ones (with only two exceptions—compounds **6** and **11**). The relationship between experimental values was linear. Moreover, good correlation between both experimental data sets was observed in the following equation:

$$\log K_w(\text{Inertsil}]) = 1.22 \log K_w(\text{IAM}) + 0.22$$
$$n = (36);\ r^2 = 0.90$$

Subsequently the calculated lipophilicity descriptors have been taken into a consideration. The values of $\log P$ calculated by means of available programs have approached value of 4.7. This means that calculated lipophilicity descriptors are significantly higher than experimental ones (this tendency is observed for the majority of the calculated values, lower values were observed mainly for imidazo derivatives). The relationships of both $\log K_w$ to all $\log P$ have shown linear character (Fig. 7). Correlation coefficients r^2s are in the range of 0.59–0.72, a better correlation was noticed for $\log K_w$ (IAM) (in the narrower range 0.68–0.72) than for $\log K_w$ (Inertsil: in the range 0.59–0.69). The best correlation was observed for $\log P$(Pallas) = f[$\log K_w$ (IAM)], the worst for $\log P$(CAChe) = f[$\log K_w$ (Inertsil)]. Presented reasoning indicates that lipophilicity descriptor $\log P$ calculated by means of Pallas program provides the best fit with experimental data in this group of compounds. It was also noticed that all programs do not differentiate the $\log P$ values calculated for

Table 7. Anticonvulsant activity and neurotoxicity of arylimidazo, pyrimido, 1,3-diazepino [2,1-*f*]purinediones

Compound[a]	MES[b,c]		ScMet[b,c]		Toxicity[b,c]		ASP class[d]
	0.5 h	4 h	0.5 h	4 h	0.5 h	4 h	
1					300 (3/4)	300[e] (1/1)	3
4					300 (1/4)	300 (1/2)	3
7					100 (2/8)		
		3					
					300 (1/4)		
8				300 (3/5)			2
9				300 (1/5)		100 (1/4)	2
10					100 (1/8)		3
					300 (1/4)		
13		100 (1/3)		[f,g]	100 (1/8)		1
	300 (1/1)	300 (1/1)					
14		100 (1/6)	300 (1/5)	100 (1/5)	100 (1/8)		1
16		100 (1/3)		300 (2/5)	100 (1/8)		1
		300 (1/1)			300 (2/4)		
20					30 (1/4)		4
				100 (1/5)	100 (2/8)		
	300 (1/1)				300 (1/4)	300 (1/2)	
21						100 (1/4)	3
						300 (1/2)	
23					100 (1/8)		2
				300 (3/5)	300 (1/4)		
24					30 (1/4)		4
					100 (1/8)	100 (1/4)	
					300 (1/4)		
25					100 (1/8)	100 (1/4)	3
					300 (1/4)	300 (2/2)	
26				300 (2/5)			2
27					100 (2/8)		3
					300 (1/4)	300 (2/2)	
28					30 (1/4)		4
					100 (2/8)	100 (1/4)	
				300 (2/5)	300 (1/4)	300 (1/2)	
29					100 (1/8)	100 (1/4)	3
30			30 (1/5)		100 (3/8)		4
			300 (3/5)	300 (1/1)	300 (4/4)	300 (2/2)	
33					100 (2/8)		3
					300 (2/4)		
34					100 (2/8)		3
					300 (4/4)	300 (2/2)	
35		300 (1/1)		30 (1/5)	100 (3/8)		1
					300 (2/4)	300 (1/2)	
36						100 (1/4)	3
37			300 (1/1)		300 (2/4)	300 (1/2)	2
38					100 (1/8)	300 (1/2)	3
					300 (2/4)		

[a] Suspension in 50% methylcellulose.
[b] Doses of 30, 100, 300 mg/kg. The figures in the table indicate the minimum dose whereby activity was demonstrated. The animals were examined 0.5 and 4.0 h after injections were made.
[c] In anticonvulsant tests figures, for example, 1/5 mean number ofanimals protected/number of animals tested; in toxicity tests—number of animals exhibiting toxicity/number of animals tested.
[d] Classification is as follows: 1—anticonvulsant activity at 100 mg/kg or less; 2—anticonvulsant activity at 300 mg/kg; 3—lack of anticonvulsant activity at 300 mg/kg, 4-neurotoxicity at dose 30 mg/kg.
[e] Death.
[f] Tonic extension.
[g] Continuous seizure activity.

constitutional isomers (compare o-, m-, and p-substituted chloro derivatives, e.g., compound **15**, **22**, and **14**) contrary to experimental methods (especially Inertsil).

The other descriptors calculated by PALLAS program, log *D*s and pK_a, were also investigated in our studies. The relation of log *D* (pH 7) = *f*(log *P*) is presented in Figure 8. It indicates that physicochemical properties for the group of derivatives with an annelated 7-membered ring are not compatible with other ones. This could also be confirmed by the distribution of log *P* versus pK_a (Fig. 8). For better illustration on that diagram

Table 8. Data of anticonvulsant test TTE in mice (ip) MES and TOX in rats (po) for compound **17**

Threshold tonic extension (TTE) test				
Mice ip dose 100 mg/kg				
0.25 h	0.5 h	1 h	2 h	4 h
2/4	0/4	1/4	2/4	1/4
MES test				
Rat po dose 30 mg/kg				
0.25 h	0.5 h	1 h	2 h	4 h
2/4	0/4	1/4	1/4	1/4
TOX test				
Rat po dose 30 mg/kg				
0.25 h	0.5 h	1 h	2 h	4 h
0/4	0/4	0/4	0/4	0/4

four quadrants (A, B, C, and D) have been chosen. The derivatives with 7-membered ring are located merely in quadrant A ($pK_a > 7.25$ and $\log P > 0$). Almost all remaining compounds are gathered in quadrant B with $\log P > 0$ and $pK_a < 7.25$.

In preliminary structure–activity studies the affinity to A_{2A} receptor was examined as a function of various lipophilicity descriptors, both experimental and calculated. Experimentally established lipophilicity of most of the active compounds is in the very broad range (depending of the method of its determination), for example (0.007–2.898 IAM, HPLC), while the theoretical lipophilicity descriptors vary in a range from −1.55 to 4.65 and they depend on the method of calculation. For the active ligands for A_{2A} ARs lipophilicity was of the order of 0.37–2.90 expressed as $\log K_w$ on IAM and −0.50 to 4.65 as $\log P$ Pallas (for the compounds active at submicromolar concentrations in the range 1.22–2.90 and 1.44–4.65, respectively). The correlation between all available lipophilicity descriptors and receptor activity for the full set of compounds was not significant. So it was concluded that the proper range of lipophilicity is not the only parameter relevant for the activity. The search for correlation of other decriptors used in QSAR with biological properties also failed.

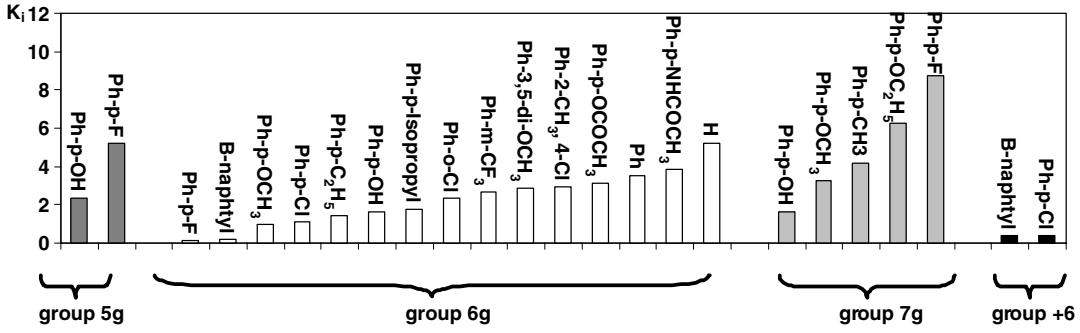

Figure 6. The affinity to adenosine A_{2A} receptor ($K_i < 25$ μM) in regard to the kind and size of annelated rings.

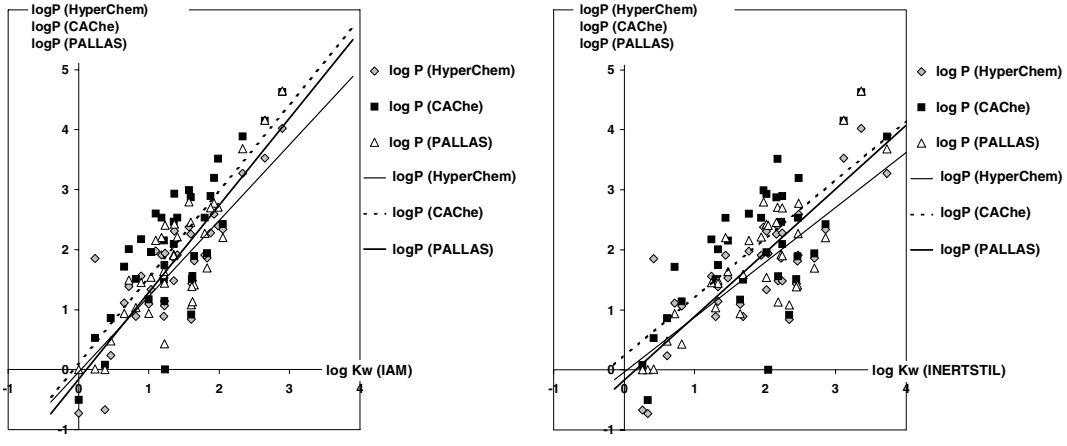

$\log P$ (HyperChem) = 1.27 $\log Kw$ (IAM) – 0.05
$r^2 = 0.69$
$\log P$ (CAChe) = 1.41 $\log Kw$ (IAM) + 0.21
$r^2 = 0.68$
$\log P$ (PALLAS) = 1.44 $\log Kw$ (IAM) - 0.24
$r^2 = 0.72$

$\log P$ (HyperChem) = 0.91 $\log Kw$ (INERTSIL) – 0.03
$r^2 = 0.62$
$\log P$ (CAChe) = 1.00 $\log Kw$ (INERTSIL) + 0.26
$r^2 = 0.59$
$\log P$ (PALLAS) = 1.16 $\log Kw$ (INERTSIL) – 0.39
$r^2 = 0.69$

Figure 7. The relations of calculated and experimental lipophilicity parameters.

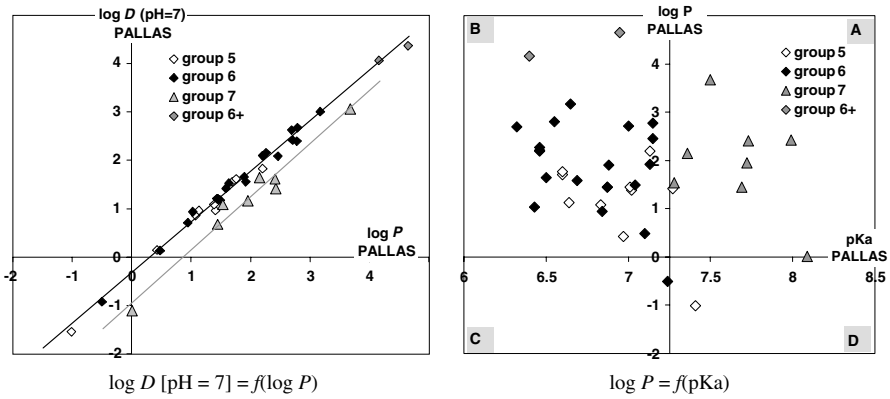

log D [pH = 7] = f(log P) log P = f(pKa)

Figure 8. Relation between descriptors calculated by means of PALLAS program.

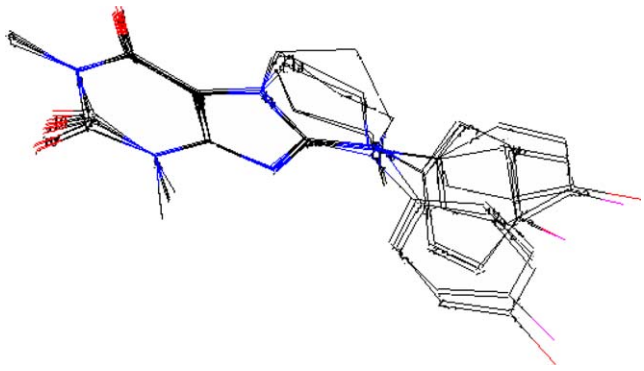

Figure 9. Superimposition of tricyclic moieties with *p*-fluoro- and *p*-hydroxyphenyl substituents obtained by means of molecular modeling.

8. 3D properties

X-ray structure analysis and molecular modeling studies allowed the following observations. The shape of all examined structures is similar: they consist of three condensed rings slightly different in the fused ring, possessing an aryl ring directly connected with this system. Aryl rings have good rotational flexibility independent of the substitution pattern of attached benzene. (compare superimposed most active compounds **7**, **23**, and **38** with para-F, and **6**, **16**, and **35** with para-OH, see Fig. 9)

However, qualitative evaluation of the electrostatic potentials of the analyzed compounds (e.g., **7** and **27**, see Fig. 10) indicates an immense influence of the kind and place of the joined aryl substituents not only on the area of the aryl ring but on the whole molecules.

9. Conclusions

A series of forty new aryl derivatives of imidazo-, pyrimido-, and 1,3-diazepino[2,1-*f*]purinediones was obtained. The new compounds tested for their adenosine receptor affinity exhibited selective affinity for adenosine A_{2A} receptors. Such a selectivity displayed by 1,3-dimethyl derivatives disappeared in the 1,3-dipropyl series. The most active compounds were found among pyrimido[2,1-*f*]purinediones. This group of compounds also showed anticonvulsant properties. Lipophilicity was not correlated with the observed pharmacological activities. It was assumed that small differences in the shape and significant changes in the electrostatic potentials,

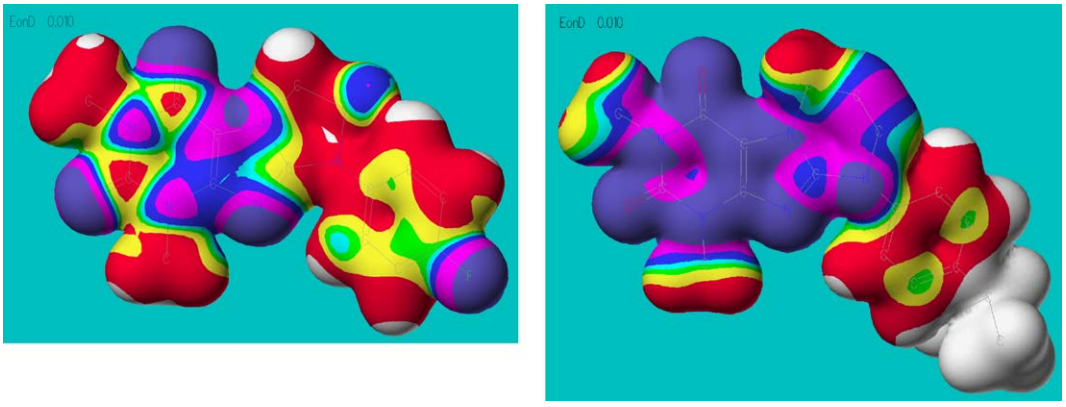

7 **27**

Figure 10. Comparison of electron density isosurfaces, colored by electroststic potentials of compounds **7** and **27** (values at the color boundaries: white, 1.0; gray, 0.8; light gray, 0.5; dark gray, 0.3; black, 0.0).

distribution of the examined molecules are responsible for the differences in activity observed in this group of compounds.

10. Experimental

10.1. Chemistry

Melting points were determinated on a MEL-TEMP II apparatus. IR spectra were taken as KBr discs on IR Specord M80 (compounds **2**–**10**) or on FT Jasco IR 410 (remaining compounds) apparatus. UV spectra were recorded on UV–vis Jena (compounds **2**–**10)** apparatus in 5×10^{-5} mol/L concentration and on Jasco UV–vis V 530 (remaining compound) in 1×10^{-5} mol/L concentration in methanol. ^{1}H NMR spectra of compounds **2**–**21** were obtained with a Bruker VM250, compound **22** with a Bruker AC200 F, and remaining compounds with a Varian-Mercury 300 MHz spectrometer with TMS as an internal standard. As solvent $CDCl_3$ was used for most of the substances, only compounds **6**, **13**, **14**, **16**, **19**, and **36** were dissolved in DMSO-d_6.

Elemental analyses (C,H, and N) were performed on a Elemental Vario-EL III apparatus and were in accordance with theoretical values within ±0.4%.

TLC data were obtained with Merck Silica Gel $60F_{254}$ aluminum sheets with A, B, C, D, E, and F developing systems. Spots were detected under UV light.

10.1.1. 7-(2-Bromoethyl)-8-bromotheophylline. A mixture of 25.8 g (100 mmol) of 8-bromotheophylline,[66] 14 g (100 mmol) of anhydrous K_2CO_3, 1 g TEBA, 19 mL (220 mmol) of 1,2-dibromoethane, and 150 mL of acetone was refluxed with stirring for 10 h. The precipitate containing unreacted 8-bromotheophylline and a small amount of 7-(2-bromoethyl)-8-bromotheophylline was filtered off. The 8-bromotheophylline was removed by stirring with NaOH. The main crop of 7-(2-bromoethyl)-8-bromotheophylline was precipitated by cooling the acetone filtrate. Total yield 77%. Mp 160–162 °C; 160 °C.[45]

10.1.2. General procedure for the synthesis of 8,9,10-arylsubstituted 1,3-dialkyl-6,7-dihydro(18*H*)-imidazo-, 6,7,8,9-tetrahydropyrimido-, 6,7,8,9-tetrahydro(10*H*)-1,3-diazepino[2,1-*f*]purine-2,4 (1*H*, 3*H*) diones (1–40) (except: 1, 11, 12, 31). A mixture of 0.73 g (2 mmol) of 7-(2-bromoethyl)-8-bromotheophylline, 0.66 g (2 mmol) of 7-(3-chloropropyl)-8-bromotheophylline (**2**), 0.79 g (2 mmol) of 7-(4-bromobutyl)-8-bromotheophylline (**3**) or 0.78 g (2 mmol) of 7-(3-chloropropyl)-8-bromo-1,3-dipropylxanthine (**6**) and corresponding amine (2–23-fold excess) was refluxed in appropriate solvent (MeDigol, EtDigol, DMF) or without solvent (compound **15**) for 5–10 h (see Table 1).

After cooling the precipitate was separated (compounds **2**, **3**, **4**, **5**, **6**, **7**, **8**, **9**, **22**, **23**, **25**, **26**, **27**, **28**, **29**, **33**, **34**, **35**, **37**, and **38**) and washed by ethanol–water or propanol–water (**32**, **39**, and **40**). Other compounds precipitated by adding water (**13**, **14**, **16**, **17**, and **20**) or ethanol (**18**, **19**) to the reaction mixture. Some compounds were separated after distillation of MeDigol and adding water (**21** and **30**) or ethanol (**15**) to the residue.

Acetyl derivatives (**24** and **36**) were prepared by refluxing compounds **16** and **35** with acetic anhydride for 5 h, removing the excess of anhydride by distillation under reduced pressure and crystallization of the residue (compound **24**) or adding water to the residue (compound **36**) and filtered off the precipitate.

All compounds were purified by crystallization (see Table 1).

10.2. Analytical HPLC measurements—determination of chromatographic lipophilicity parameters

The chromatographic system used consisted of a Model L-6200A pump, a Model L-4250 UV–vis detector, and a Model D-2500 chromato-integrator (all from Merck-Hitachi, Vienna, Austria). Two HPLC columns were employed: Inertsil ODS-3 octadecylsilica column 150×4.6 mm id, particle size 5 μm, purchased from GLC Sciences Inc., Tokyo, Japan, and the so-called immobilized artificial membrane column IAM.PC.C0/C3 150×4.6 mm id, particle size 12 μm, purchased from Regis Chemical Company, Morton Grove, IL, USA. A Rheodyne (Cotati, CA, USA) Model 7215 injecting valve fitted with a 20 μL sample loop was used.

The experiments were carried out isocratically. The HPLC retention factors, k, on Inertsil ODS-3 column were determined for four to six compositions of acetonitrile–0.1 M Tris buffer (pH 7.4) mobile phase ranging from 70:30 to 30:70 (v/v). The mobile phase flow rate was 1.5 mL/min. On IAM column k values for the compounds studied were determined for four to five compositions of acetonitrile-universal buffer mobile phase (pH 7.0) ranging from 50:50 to 20:80 (v/v). The mobile phase flow rate was 1 mL/min.

The experiments on both columns were performed at ambient temperature. The detection wavelength was 280 nm and the dead volume was determined by a signal of sodium nitrate. The mobile phases used were filtered through a GF/F glass microfiber filter (Whatman, Maidstone, UK) and degassed by ultrasonication before use. The compounds were dissolved in methanol.

The logarithms of the HPLC retention factors, $\log k$, for individual compounds analyzed in a given chromatographic system were regressed against the volume fraction of organic modifier in the mobile phase. The linear part of the relationship was extrapolated to a hypothetical retention factor corresponding to 100% buffer in the mobile phase. Finally, the retention parameters normalized to pure buffer, $\log K_w$, were obtained.

10.3. Pharmacology

10.3.1. Adenosine receptor binding assays. Adenosine receptor binding assays were performed as previously described using rat brain cortical membrane preparations for A_1 AR assays and rat brain stratial membrane preparations for A_{2A} assays.[67–69] Frozen rat brains (unstripped) were obtained from Pel-Freez®, Rogers, Arkansas, USA. For assays at human A_1, A_{2A}, A_{2B}, and A_3 ARs, CHO cell membranes containing the human receptors were used as described.[57,67] [^{3}H]2-chloro-N^6-cyclopentyladenosine ([^{3}H]CCPA) was used as the A_1 radioligand, [^{3}H]3-(3-hydroxypropylo)-7-methyl-8-(*m*-methoxystyryl)-1-propargylxanthine ([^{3}H]MSX-2) as the A_{2A} radioligand[58], [^{3}H]4-(2-[7-amino-2-(2-furyl)-[1,2,4]triazolo[2,3-*a*][1,3,5]-triazin-5-4-(amino)-ethyl)phenol ([^{3}H]ZM241385) as the A_{2B} receptor radioligand[59], and [^{3}H]-phenyl-8-ethyl-4-methyl-(8*R*)-4,5,7,8-tetrahydro-1*H*-imidazo-[2,1-*i*]-purine-5-one ([^{3}H]PSB-11) as the A_3 AR radioligand.[16] Initially, a single high concentration of compound (25 μM at A_1 and A_{2A}, 10 μM at A_{2B} and A_3 receptors) was tested in three (A_1, A_{2A}) or two (A_{2B}, A_3) independent experiments. For potent compounds, curves were determined using six to seven different concentrations of test compounds spanning 3 orders of magnitude. Data were analyzed using the PRISM program version 3.0 (Graph Pad, San Diego, CA, USA).

10.3.2. Anticonvulsant screening. The anticonvulsant evaluation was carried out using reported procedures.[62,63] Male albino mice (F-1 strain, 18–25 g) were used as experimental animals. For testing compound **17** male albino rats (Sprague–Dawley 100–150 g) were used. Groups of 1–5 mice were used in MES, scMet, and TTE tests, group of 2–8 animals in rotorod test. For the evaluation of activity after oral administration, groups of 4 rats were used. The tested compounds were suspended in a 0.5% methylcellulose–water mixture. In the preliminary screening each compound was administered as an ip injection at three dose levels (30, 100, and 300 mg/kg) with anticonvulsant activity and neurotoxicity assessed at 0.5 and 4 h intervals after administration. In the TTE test also intervals of 0.25, 1, and 2 h were applied. Anticonvulsant efficacy was measured by maximal electroshock (MES) and subcutaneous pentylenetetrazole (scMet), neurological deficit was investigated in the rotorod test; the data are presented in Table 7. The TTE test for compound **17** is presented in Table 8. Compound **17** was examined for oral activity in the rat MES and neurotoxicity screen at a dose of 30 mg/kg (Table 8).

10.4. X-ray structure analysis of 37 and 40

Crystal data for **37**: $C_{18}H_{21}N_5O_3$; mol. mass 355.40; monoclinic; space group: $C2/c$; $a = 15.0201(18)$ Å; $b = 8.0775(18)$ Å; $c = 28.449(4)$ Å; $\beta = 28.449(4)°$; $V = 3449.8(10)$ Å^3; $z = 8$; d$x = 1.369$ mg/m^3; $\mu = 0.096$ mm^{-1}; $F(000) = 1504$; final $R = 0.075$ for 3025 reflections [$I > 4\sigma(I)$].

Crystal data for **40**: $C_{20}H_{24}ClN_5O_2\ xH_2O$; mol. mass 419.91; monoclinic; space group: $P2_1/c$; $a = 10.054(4)$ Å; $b = 4.828(3)$ Å; $c = 42.267(12)$ Å; $\beta = 96.75(3)°$; $V = 2037.5(5)$ Å^3; $z = 4$; d$x = 1.429$ mg/m^3; $\mu = 0.022$ mm^{-1}; $F(000) = 888$; final $R = 0.084$ for 1900 reflections [$I > 4\sigma(I)$].

The crystals of **37** and **40** were obtained by slow evaporation of ethanol solution. The measurement of the crystals was performed on a Kuma4CCD κ-axis diffractometer with graphite-monochromated MoKα radiation at room temperature. The data were corrected for Lorentz and polarization effects. No absorption correction was applied. The structures were solved by direct methods[70] and refined using SHELXL.[71] The full-matrix least-squares refinement was based on F^2. The positions of all H-atoms were found from electron density $\Delta\rho$ map and refined in raiding model with the isotropic displacement parameters of 1.5 times the respective U_{eq} values for the parent-atoms. Atomic scattering factors were those as in SHELXL.[71] Crystallographic data (excluding structural factors) for the structures reported in this paper have been deposited with the Cambridge Crystallographic Data Center and allocated the deposition numbers: CCDC 289057 for **37** and CCDC 289056 for **40**. Copies of the data can be obtained free of charge on application to CCDC, 12 Union Road, Cambridge CB2 1EW, UK (Fax: Int code +1223 336 033; E-mail: deposit@ccdc.cam.ac.uk).

Acknowledgments

The authors are grateful to Professor James Stables for providing the biological data through the ADD Program of the National Institute of Neurological and Communicative Disorders and Stroke at the National Institutes of Health, Bethesda, MD, USA. This study was supported by Polish State Committee for Scientific Research (Grant No. 6 P05F 024 21) and by the Deutsche Forschungsgemeinschaft (GRK 677).

Supplementary data

Supplementary data associated with this article can be found, in the online version, at doi:10.1016/j.bmc.2006.06.052.

References and notes

1. Fredholm, B. B.; IJzerman, A. P.; Jacobson, K. A.; Klotz, K. N.; Linden, J. *Pharmacol. Rev.* **2001**, *53*, 527.
2. Hess, S. *Exp. Opin. Ther. Patent* **2001**, *11*, 1533.
3. Dhalla, A. K.; Shryock, J. C.; Shreeniwas, R.; Bellardinelli, L. *Curr. Top. Med. Chem.* **2003**, *3*, 369.
4. Poulsen, S.-A.; Quinn, R. J. *Bioorg. Med. Chem.* **1998**, *6*, 619.
5. Müller, C. E. *Farmaco* **2001**, *56*, 77.
6. Müller, C. E. *Exp. Opin. Ther. Patents* **1997**, *7*, 419.
7. Müller, C. E. *Drugs Future* **2000**, *25*, 1043.

8. Baraldi, P. G.; Tabrizi, M. A.; Bovero, A.; Avitabile, B.; Preti, D.; Fruttarolo, F.; Romagnoli, R.; Varani, K.; Borea, P. A. *Eur. J. Med. Chem.* **2003**, *38*, 367.
9. Feoktistov, I.; Palosa, R.; Holgate, S. T.; Biaggioni, I. *Trends Pharmacol. Sci* **1998**, *19*, 148.
10. Fiebich, B. L.; Biber, K.; Gyufko, K.; Berger, M.; Bauer, J.; Van Calker, D. *J. Neurochem.* **1996**, *66*, 1426.
11. Harada, H.; Asano, O.; Hoshino, Y.; Yoshikawa, S.; Matsukura, M.; Kabasawa, Y.; Niijima, J.; Kotake, Y.; Watanabe, N.; Kawata, T.; Inoue, T.; Horizoe, T.; Yasuda, N.; Minami, H.; Nagata, K.; Murakami, M.; Nagaoka, J.; Kobayashi, S.; Tanaka, I.; Abe, S. *J. Med. Chem.* **2001**, *44*, 170.
12. Müller, C. E. *Curr. Top. Med. Chem.* **2003**, *3*, 445.
13. Müller, C. E. *Mini-Rev. Med. Chem.* **2001**, *1*, 417.
14. Kieć-Kononowicz, K.; Drabczyńska, A.; Pękala, E.; Michalak, B.; Müller, C. E.; Schumacher, B.; Karolak-Wojciechowska, J.; Duddeck, H.; Rockitt, S.; Wartchow, R. *Pure Appl. Chem.* **2001**, *73*, 1411.
15. Weyler, S.; Hayallah, A. M.; Müller, C. E. *Tetrahedron* **2003**, *59*, 47–54.
16. Müller, E. C.; Diekmann, M.; Thorand, M.; Ozola, V. *Bioorg. Med. Chem. Lett.* **2002**, *12*, 501.
17. Ozola, V.; Thorand, M.; Diekmann, M.; Qurishi, R.; Schumacher, B.; Jacobson, K. A.; Müller, C. E. *Bioorg. Med. Chem.* **2003**, *11*, 347.
18. Cacciari, B.; Pastorin, G.; Spalluto, G. *Curr. Top. Med. Chem.* **2003**, *3*, 403.
19. Shimada, J.; Suzuki, F.; Nokada, H.; Ishii, S.; Ichikawa, S. *J. Med. Chem.* **1992**, *36*, 2342.
20. Müller, C. E.; Stein, B. *Curr. Pharm. Des.* **1996**, *2*, 501.
21. Jacobson, K. A.; Nikodijevic, O.; Padgett, W. L.; Gallo-Rodriguez, C.; Maillard, M.; Daly, J. W. *FEBS Lett.* **1993**, *323*, 141.
22. Grondin, R.; Bédard, P. J.; Hadj Tahar, A.; Grégoire, L.; Mori, A.; Kase, H. *Neurology* **1999**, *52*, 1673.
23. Kanda, T.; Jackson, M. J.; Smith, L. A.; Pearce, R. K. B.; Nakamura, J.; Kase, H.; Kuwana, Y.; Jenner, P. *Ann. Neurol.* **1998**, *43*, 507.
24. Jacobson, K. A.; Gallo-Rodriguez, C.; Melman, N.; Fischer, B.; Maillard, M.; Van Bergen, A.; Van Galen, P. J. M.; Karton, Y. J. *J. Med. Chem.* **1993**, *36*, 1333.
25. Shimada, J.; Koike, N.; Nonaka, H.; Shiozaki, S.; Yanagawa, K.; Kanda, T.; Kobayashi, H.; Ichimura, M.; Nakamura, J.; Kase, H.; Suzuki, F. *Bioorg. Med. Chem. Lett.* **1997**, *7*, 2349.
26. Knutsen, L. J. S.; Weiss, S. M. *Curr. Opin. Invest. Drugs* **2001**, *2*, 668.
27. Rabasseda, X.; Sorbera, L. A.; Martin, L.; Leeson, P. A.; Castañer, J. *Drugs Future* **2001**, *26*, 20.
28. Kanda, T.; Jackson, M. J.; Smith, L. A.; Pearce, R. K. B.; Nakamura, J.; Kase, H.; Kuwana, Y.; Jenner, P. *Exp. Neurol.* **2000**, *162*, 321.
29. Jenner, P. *Neurology* **2003**, *61*, S101.
30. Kase, H.; Aoyama, S.; Ichimura, M.; Ikeda, K.; Ishii, A.; Kanda, T.; Koga, K.; Koike, N.; Kurokawa, M.; Kuwana, Y.; Mori, A.; Nakamura, J.; Nonaka, H.; Ochi, M.; Saki, M.; Shimada, J.; Shindou, T.; Shiozaki, S.; Suzuki, F.; Takeda, M.; Yanagawa, K.; Richardson, P. J.; Jenner, P.; Bedard, P.; Borrelli, E.; Hauser, R. A.; Chase, T. N. *Neurology* **2003**, *61*, S97.
31. Petzer, P. J.; Steyn, S.; Castagnoli, K. P.; Chen, J.-F.; Schwarzschild, M. A.; Van der Schyf, J. C.; Castagnoli, N. *Bioorg. Med. Chem.* **2003**, *11*, 1299.
32. Pintor, A.; Quarta, D.; Pezzola, A.; Reggio, R.; Popoli, P. *Eur. J. Pharmacol.* **2001**, *421*, 177.
33. Popoli, P.; Pintor, A.; Domenici, M. R.; Frank, C.; Tebano, M. T.; Pezzola, A.; Scarchilli, L.; Quarta, D.; Reggio, R.; Malchiodi-Albedi, F.; Falchi, M.; Massotti, M. *J. Neurosci.* **2002**, *22*, 1967.
34. Bastia, E.; Varani, K.; Monopoli, A.; Bertorelli, R. *Neurosci. Lett.* **2002**, *328*, 241.
35. Müller, C. E.; Geis, U.; Hipp, J.; Schobert, U.; Frobenius, W.; Pawłowski, M.; Suzuki, F.; Sandoval-Ramirez, J. *J. Med. Chem.* **1997**, *40*, 4396.
36. Müller, C. E.; Sandoval-Ramirez, J.; Schobert, U.; Geis, U.; Frobenius, W.; Klotz, K. N. *Bioorg. Med. Chem.* **1998**, *6*, 707.
37. Sauer, R.; Maurinsh, J.; Reith, U.; Fülle, F.; Klotz, K. N.; Müller, C. E. *J. Med. Chem.* **2000**, *43*, 440.
38. Jackson, E. K.; Herzer, W. A.; Suzuki, F. *J. Pharmacol. Exp. Ther.* **1993**, *267*, 1304.
39. Müller, C. E.; Maurinsh, J.; Sauer, R. *Eur. J. Pharm. Sci.* **2000**, *10*, 259.
40. Holschbach, M. H.; Olsson, R. A. *Curr. Pharm. Des* **2002**, *8*, 2345.
41. Hockemeyer, J.; Burbiel, J. C.; Müller, C. E. *J. Org. Chem.* **2004**, *69*, 3308.
42. Nonaka, Y.; Shimada, J.; Nonaka, H.; Koike, N.; Aoki, N.; Kobayashi, H.; Kase, H.; Yamaguchi, K.; Suzuki, F. *J. Med. Chem.* **1993**, *36*, 3731.
43. Drabczyńska, A.; Schumacher, B.; Müller, C. E.; Karolak-Wojciechowska, J.; Michalak, B.; Pękala, E.; Kieć-Kononowicz, K. *Eur. J. Med. Chem.* **2003**, *38*, 397.
44. Drabczyńska, A.; Müller, C. E.; Schumacher, B.; Karolak-Wojciechowska, J.; Pękala, E.; Kieć-Kononowicz, K. *Bioorg. Med. Chem.* **2004**, *12*, 4895.
45. Cacace, F.; Masironi, R. *Ann. Chim. (Roma)* **1956**, *46*, 806.
46. Rockitt, S.; Wartchow, R.; Duddeck, H.; Drabczyńska, A.; Kieć-Kononowicz, K. *Z. Naturforsch.* **2001**, *56b*, 319.
47. Pawłowski, M.; Drabczyńska, A.; Gorczyca, M.; Malec, D.; Modzelewski, J. *Acta Pol. Pharm.—Drug Res.* **1994**, *51*, 385.
48. Eckstein, M.; Drabczyńska, A. *Synthesis* **1979**, *8*, 581.
49. Eckstein, M. *Dissert. Pharm.* **1962**, *4*, 435.
50. Bergmann, F.; Dickstein, S. *J. Am. Chem. Soc.* **1955**, *77*, 691.
51. Rybár, A.; Antoš, K. *Coll. Czech. Chem. Commun.* **1970**, *35*, 1415.
52. Cremer, D.; Pople, J. A. *J. Am. Chem. Soc.* **1975**, *97*, 1354.
53. Evans, G. G.; Boeyens, J. A. *Acta Crystallogr.* **1989**, *B45*, 581.
54. HyperChem ver. 6.0.
55. CAChe ver. 6.1, Fujitsu (2000–2003).
56. Pallas Program, Ver. 1.2, CompuDrug International Inc. (1994).
57. Klotz, K.-N.; Hessling, J.; Hegler, J.; Owman, C.; Kull, B.; Fedholm, B. B.; Lohse, M. J. *Naunyn-Schmiedeberg's Arch. Pharmacol.* **1998**, *357*, 1.
58. Müller, C. E.; Maurinsh, J.; Sauer, R. *Eur. J. Pharm. Sci* **2000**, *10*, 259.
59. Ji, X-D.; Jacobson, K. A. *Drug Des. Discov.* **1999**, *16*, 217.
60. Gao, Z. G.; IJzerman, A. P. *Biochem. Pharmacol.* **2000**, *60*, 669.
61. Yan, L.; Müller, C. E. *J. Med. Chem.* **2004**, *47*, 1031.
62. Kupferberg, H. J. *Epilepsia* **1989**, *30*, S51.
63. Stables, J. P.; Kupferberg, H. J. National Institute of Neurological Disorders and Stroke. Anticonvulsant Screening Project Raport. Chapter 16. www.ninds.nih.gov/about_ninds/anticonvulsant_screening_project.htm.
64. LeTiran, A.; Stables, J. P.; Kohn, H. *J. Med. Chem.* **2002**, *45*, 4762.
65. McGaraughty, S.; Cowart, M.; Jarvis, M. F.; Berman, R. F. *Curr. Top. Med. Chem.* **2005**, *5*, 43.
66. Eckstein, M.; Gorczyca, M.; Zejc, A. *Acta Pharm. Jugosl.* **1972**, *11*, 133.
67. Müller, C. E.; Thorand, M.; Quirshi, R.; Dieckmann, M.; Jacobson, K. A.; Padgett, W. L.; Daly, J. W. *J. Med. Chem.* **2002**, *45*, 3440.

68. Hess, S.; Müller, C. E.; Frobenius, W.; Reith, U.; Klotz, K.-N.; Eger, K. *J. Med. Chem.* **2000**, *43*, 4636.
69. Hayallah, A. M.; Sandoval-Ramirez, J.; Reith, U.; Schobert, U.; Preiss, B.; Schumacher, B.; Daly, J. W.; Müller, C. E. *J. Med. Chem.* **2002**, *45*, 1500.
70. Sheldrick, G. M. SHELXTL PC^{MT}, Siemens Analytical X-Ray Instruments Inc., Madison, Wisconsin, USA, 1990.
71. Sheldrick, G. M. SHELXL-93. A FORTRAN-77 Program for the Refinement of Crystal Structures from Diffraction Data. University of Göttingen, Germany, 1993.